Ternary Regime Switching Modelling for Financial Asset Price Data

A Thesis

submitted to
Indian Institute of Science Education and Research Pune
in partial fulfillment of the requirements for the
BS-MS Dual Degree Programme

by

D.V.S. Abhijit
20161005

Indian Institute of Science Education and Research Pune
Dr. Homi Bhabha Road,
Pashan, Pune 411008, INDIA.

June, 2021

Supervisor: Dr. Anindya Goswami
© D.V.S. Abhijit 2021

Certificate

This is to certify that this dissertation entitled Ternary Regime Switching Modelling for Financial Asset Price Data towards the partial fulfilment of the BS-MS dual degree programme at the Indian Institute of Science Education and Research, Pune represents study/work carried out by D.V.S. Abhijit at Indian Institute of Science Education and Research under the supervision of Dr. Anindya Goswami, Associate Professor, Department of Mathematics , during the academic year 2020-2021.
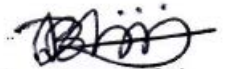
Dr. Anindya Goswami

Committee:

Dr. Anindya Goswami

GKB

Dedicated to Amma and Naanna.

Declaration

I hereby declare that the matter embodied in the report entitled Ternary Regime Switching Modelling for Financial Asset Price Data are the results of the work carried out by me at the Department of Mathematics, Indian Institute of Science Education and Research, Pune, under the supervision of Dr. Anindya Goswami and the same has not been submitted elsewhere for any other degree.

D.V.S. Abhijit

Acknowledgements

I would like to express my earnest and heartfelt gratitude to my mentor Dr. Anindya Goswami for his invaluable advice, guidance and encouragement throughout the project. The time and effort he has invested in my project are one of the major reasons for this thesis taking shape. I am thankful to Dr. Gopal K. Basak, my thesis committee member, for his inputs and guidance during the project.

I am indebted to my parents for the constant support and being a source of impetus during the course of the project. I am grateful for my grand parents for backing me always. I also would like to thank the forces of nature for being kind to me and enabling me to finish the project on time.

x

Abstract

In this project a ternary regime Markov switching jump diffusion model for financial asset price data is proposed. Initially, we propose a statistical technique for the detection of jumps and volatility estimation in a return time series data using a threshold method. As the threshold and volatility estimator are derived together by solving an implicit equation, this leads to unprecedented accuracy in jump detection over wide-ranging parameter values. Next, using the proposed threshold method the increments attributed to jumps are removed from historical data of various Indian sectoral indices. Thereafter, we attempt to model the derived continuous part of the data by analysing the presence of regime switching dynamics in the volatility coefficient using discriminating statistics, proposed by us, which are sensitive to the transition kernel of the regime switching model.In particular we have restricted ourselves to ternary regime switching dynamics. Finally, the performance of the proposed regime switching model is tested by examining its replication of the empirical Cumulative Distribution Function(eCDF) of the return time series.

Contents

Chapter 1

Introduction

Stock prices possess an inherent randomness. Attempts have been made to model the dynamics of stock price using diffusion processes. In 1973, Black, Scholes and Merton, [17], used Geometric Brownian Motion to model Stock/Risky Asset prices. This is the pioneering asset pricing model that continues to influence all models to this day. The theoretical results obtained from this model were not consistent with empirical observations.Various assumptions made by the model such as constant market parameters such as volatility, drift and interest rate turned out to be unrealistic since in the real world these parameters are ever changing. Many Models have been developed to address to the inconsistency between theory and empirical observations and issue of assumptions made by the Black, Scholes and Merton model. A few examples are the Heston Model and several regime switching models.
The Heston Model[15] considers volatility to be a stochastic process unlike the Black, Scholes and Merton model. It makes the use of a Cox Ingersoll Ross(CIR) process to model the volatility of a stock. Modeling of volatility as a CIR process implies volatility to follow mean reverting dynamics. Many models later have extended the Heston Model in various forms.

The phenomenon of quick or rapid variations in stock prices(where the historical volatility is too high or too low) due to certain events that occur rarely cannot be explained by models with continuous path such as the Black, Scholes and Merton model and the Heston Model. The real time series data of financial asset prices do exhibit jump discontinuities which cannot be explained by a diffusion model alone. The sudden large changes in the return series are attributed to jump discontinuities.To address the phenomenon of empirically observed big and sudden changes in simple return series the market jump diffusion models have been considered. Merton[49] in 1976 introduced a pioneering jump diffusion option pricing model. Other examples of jump diffusion models are [24] and [25]. These models introduce the concept of discontinuity into the stock price dynamics. A jump diffusion extension of a geometric Brownian motion is called a geometric Lévy process. It intends to improve over the geometric Brownian motion process of the BSM model. This model is used in [28]. Models also have been developed by introducing jump into the Heston Model. An example is [30].

Regime switching models are another type of models gaining traction in literature of Mathematical Finance after the work of of Hamilton (1989) [14] and Di Masi et.al (1994) [13]. There have been regime switching extensions

of the Black, Scholes and the Heston Model. These models allow variation of Market parameters in a simplistic manner. In Regime switching models, the key market parameters evolve as finite state pure jump process such as a Markov chain. The volatility and drift coefficients are changed based on the movement of a unobserved pure jump process. One such regime switching model is a Markov Modulated Geometric Brownian Motion(MMGBM), which is a Geometric Brownian motion whose parameters evolve as Markov chain. As research in the regime switching field grew, the models also gained popularity academically. After [13] various researchers assumed regime switching models for asset price dynamics. Examples of such regime switching models are [1], [2], [3], [4], [5], [6], [7] [8], [9], [10], [11], [12]. Some examples of regime switching models modulated by a Markov chain are[18], [19] and [20]. Regime switching extension of the Heston model is studied in [16]. The list is just indicative and not exhaustive.

The jump diffusion models or regime switching models alone have not been able to model and explain various aspects of the asset price dynamics. Therefore,this thesis aims at a unified inference of jump diffusion models with regime switching. In this thesis, the inference problem for a class of Ternary regime-switching jump diffusion model is studied. In [33], the statistical inference of a class of binary regime-switching jump diffusion model of financial time series data studied. In [33] a particular type of test statistics has been used which is suitable for a model where the low volatility regime occurs with a low probability and high volatility regime occurs with low probability, not together, but in isolation. An extension of that study where models where, the high volatility regime and low volatility regime occur with low probability together is considered in this thesis. The jumps are identified and removed before inferring the regimes in the regime-switching volatility dynamics.

Various approaches have been studied to infer the parameters of jump models which include the maximum likelihood approach [35], the Markov chain Monte Carlo approach [39], and threshold estimators [40], [43]. In, [32] jump discontinuities are inferred using a Maximum Likelihood Estimation(MLE) approach while [43] and [31] a non parametric approach is used for jump detection. Specifically, [31] infers jump discontinuities by minimizing the Mean Square Error(MSE). In this thesis a threshold technique is proposed, to disentangle the jump from the continuous part. In this method we obtain a threshold that is dependent on the volatility coefficient.

The standard threshold method involves fixing a threshold value of return, based on the time granularity of the data, and a jump is said to have occurred when the return crosses that threshold and the instances when the jump has occurred are classified as the jump times. The volatility coefficient is estimated post the removal of the jumps detected, from the return series. One must note that, if the threshold does not depend on the diffusion coefficient, the jump identification is poor for a large value of the volatility coefficient due to rare but large increments caused by Brownian motion, would be misclassified as jumps. This issue has been addressed by us, by simultaneously obtaining the threshold and the volatility estimator, by solving an implicit equation. The maximum solution is obtained by an iterative scheme that rapidly converges to it. The resulting estimator is denoted as the maximal estimator, as it maximizes the contribution of diffusion term in explaining return series and reduces the false-positive error. Post the removal of jumps detected from the return series, the continuous part of the data(return series)is modelled using a ternary regime switching GBM model.

Discriminating statistics proposed by us, are used to test the model. The sampling distribution of the discriminating statistics varies drastically and desirably, with varying choices of instantaneous rate parameter in the regime switching dynamics. The discriminating statistics are constructed using certain descriptive statistics of squeeze and expansion duration of the Bollinger band. The sampling distribution of the descriptive statistics of these durations,

under a particular model hypothesis, do not have a form by which analytical inference can be done. Despite this, the empirical distribution of the statistics can be obtained using a reliable simulation procedure. This is a standard approach known as the typical realization surrogate data approach in Theiler et al. [47]. Other works such as [45] and [46] use a similar approach. As the approach in [33] serves as a bedrock for this thesis.

This thesis is organised into chapters with several sections and subsections within the chapters. Chapter 2 provides a brief picture and describes diffusion, jump diffusion and Markov switching models for asset price dynamics developed to date. In Chapter 3, we propose the development of a method for inference of jumps in uni-regime and regime switching Merton's jump diffusion model. In Chapter 4, method of obtaining squeeze and expansion durations is given. These durations are used to propose discriminating statistics which are detailed in the same chapter. The rejection procedure of any composite null hypothesis based on these statistics is also elucidated in Chapter 4. The discretization of a few important class of regime switching models is explained in cChapter 5. Chapter 6 deals with the application of the proposed inference technique developed to some empirical data and some numerical experiments on the best fit models to test their performance.

Chapter 2

Stochastic Models of Asset Price Dynamics

2.1 Diffusion and Jump diffusion models

In 1973, Black, Scholes and Merton [17] used Geometric Brownian Motion to model Stock/Risky Asset prices. It is known as the Black Scholes Merton(BSM)model which is given by the following stochastic differential equation:

$$dS_t = dS_t(\mu dt + \sigma dW_t),$$

where S_t is the price of the stock, $S_0 > 0$, μ is the drift(expected return) of the stock and σ is the volatility of the stock(standard deviation) and W_t is standard Brownian Motion.

The theoretical results, obtained from the model were not consistent with empirical observations due to various assumptions of the model such as constant market parameters such as volatility, drift and interest rate which were unrealistic as, in the real world these parameters are constantly changing. Further, Models have been developed to address to the inconsistency between theory and empirical observations mainly due to the assumptions made by the Black, Scholes and Merton model. A few examples are the Heston Model and several regime switching models.

The Heston Model[15] considers volatility to be a stochastic process unlike the Black, Scholes and Merton model. It makes the use of a Cox Ingersoll Ross(CIR) process to model the volatility of a stock. Modeling of volatility as a CIR process implies volatility to follow mean reverting dynamics. Various successive models have extended the Heston Model in different forms . The Heston Model is given by the following Stochastic differential equations:

$$dS_t = \mu S_t + \sqrt{v_t} S_t dW_t$$
$$dv_t = \kappa(\theta - v_t)dt + \sigma\sqrt{v_t}dW_t',$$

4

W and W' are standard Brownian motions, such that $dW_t dW_t' = \rho dt$, S_t is the price of the stock, v_t is the volatility of the stock. The parameters of volatility are defined as follows: κ is speed, θ is the long run mean, and σ is the volatility of volatility. The system of differential is also subject to additional conditions as: Feller condition: $\sigma^2 < 2\kappa\theta$, which assures the non negativity of v and to assure square integrability of S: $\sigma \leq \frac{\kappa}{(2\rho+\sqrt{2})^+}$.

As discussed in the introduction, to address the phenomenon of quick or rapid variations in stock prices due to certain events that occur rarely in the market jump diffusion models have been considered. Sudden large changes in the return series are attributed to jump discontinuities. Some examples of jump diffusion models are [24] and [25]. These models introduce the concept of discontinuity into the stock price dynamics. One example of a jump diffusion process is :

$$dS_t = S_{t^-}(\mu dt + \sigma dW_t + \int \eta(z)N(dt, dz)),$$

where, $\eta : \mathbb{R} \to \mathbb{R}$ is continuous and bounded above and $\eta(z) > -1$ and $N(dt, dz)$ is a Poisson random measure with intensity $\nu(z)dt$, where ν is a finite Borel measure. [24] and [25] study similar models as above .

A jump diffusion extension of a geometric Brownian motion is called a geometric Lévy process. It intends to improve over the geometric Brownian motion process of the BSM model. It is given by:

$$S_t = S_0 \exp Z_t, \text{ where } Z_t \text{ is a Lévy process.}$$

$Z_t = \sigma W_t + Y_t$, where W_t is a standard Brownian motion and Y_t is jump Lévy process independent of W_t.
The process Y_t has the following representation in terms of the Poisson random Measure, $N(dt, dz)$, $t \geq 0$, z$\in \mathbb{R} \setminus \{0\}$ generated by the jumps of Z_t:

$$Y_t = bt + \int_0^t \int_{\mathbb{R} \setminus \{0\}} z I_{|z| \geq 0} N(ds, dz) + \int_0^t \int_{\mathbb{R} \setminus \{0\}} z I_{|z| < 0} [N(ds, dz) - \nu(dz)ds] \text{ and } I \text{ is the indicator function.}$$

Here, $\nu(dz)$ is the Lévy measure which satisfies the following conditions: $\int \min(z^2, 1)\nu(dz) < \infty$. This model is used in [28].
Models also have been developed by introducing jump into the Heston Model. An example is [30]. The model is as follows:

$$dS_t = (r_t - d_t - \gamma m^j)S_t + \sqrt{v_t}S_t dW_t^s + (e^{J^s} - 1)S_t dN_t^p, \ S_0 = s,$$
$$dv_t = \kappa(\theta - v_t)dt + \sigma\sqrt{v_t}dW_t^v + J^v dN_t^p, \ V_0 = v$$

where, W^s and W^v are standard Brownian motions, such that $dW_t^s dW_t^v = \rho dt$, N^p is a Poisson process with constant intensity γ, J^s is called the return jump and J^v is called the variance jump.
Amplitude of return jump is assumed to have normal distribution and Amplitude of volatility jump is assumed to have exponential distribution as follows:

$$\overline{\omega^s} = \frac{1}{2\pi\delta^2}\exp\left(-\frac{(J^s-\nu)^2}{2\delta^2}\right), \quad \overline{\omega^v} = \frac{1}{\eta}\exp\left(-\frac{-1}{\eta}J^v\right),$$

where, ν is the mean and δ is the volatility of return jump J^s and η is the mean of variance jump J^v.

$$m^j = \exp(\nu + \tfrac{1}{2}\delta^2) - 1, \text{ is the compensator.}$$

2.2 Markov Switching Models

In Regime switching models market parameters vary with the changing state of economy which in turn is modulated by a Markov or a Semi Markov chain. Some examples of regime switching models modulated by a Markov chain are[18], [19] and [20].

Regime switching was integrated into the BSM model to address some of the shortcomings. It is called the Markov Modulated Geometric Brownian Motion(MMGBM)model. The stochastic differential equation of the MMGBM model is as given below:

$$dS_t = \mu(X_t)S_t dt + \sigma(X_t)S_t dW_t$$

where $\{X_t\}_{t\geq 0}$, is a Markov process independent of the stock price S_t. τ is the time-index set $\{0,1,2,3,...\}$, $(\Omega, \mathcal{F}, \mathcal{P})$, the probability space and $\mathcal{X} = \{1,2,3,...,k\}$ be the state-space of an irreducible k state Markov-chain.

The transition rate matrix of the Markov chain is λ, where, $\lambda_{ij} \geq 0 \; for \; i \neq j \; \& \; \lambda_{ii} = -\sum_{j\neq i}^{k} \lambda ij$, i, j $\in \mathcal{X}$

$p_{ij} = \frac{\lambda_{ij}}{|\lambda_{ii}|}$ are the transition probabilities from state i to state j, where $i \neq j$ and $p_{ii} = 0$.

In Markov Modulated Geometric Brownian motion the drift of the stock μ and the volatility of the stock σ are assumed to evolve as a function of a continuous time Markov chain. The stochastic differential equation of MMGBM is as given below,

$$dS_t = \mu(X_t)S_t dt + \sigma(X_t)S_t dW_t \tag{2.2.1}$$

where, $\{X_t\}_{t\geq 0}$, is a Markov process independent of the stock price, $\mu(X_t)$, $\sigma^2(X_t)$ are the Markov dependent drift and volatility of the stock respectively and $\{W_t\}_{t\geq 0}$ is standard Brownian Motion.

Definition 2.2.1. *The stock price in a Markov Modulated Brownian motion is given as follows:*

Let the initial stock price at t=0 be $S_0 = s$. Then the stock price at any time t=T', is given as,

$$S_{T'} = S_0 exp[\int_0^{T'} \mu(X_t) - \sigma^2(X_t)/2)]dt + \int_0^{T'} \sigma(X_t)dW_t.$$

Some examples of MMGBM models are [1], [13], [18], [19], [20], [21], [22] and [23].

Regime switching extension of the Heston model is studied in [16]. It intends to address several inconsistencies of theoretical results of the Heston model with real/empirical data. The model is as follows:

$$dS_t = \mu S_t + \sqrt{v_t} S_t dW_t,$$
$$dv_t = \kappa(X_t)(\theta(X_t) - v_t)dt + \sigma(X_t)\sqrt{v_t}dW_t{}', V_0 = v_0,$$

where, X_t is a homogeneous continuous time Markov chain, W and W' are standard Brownian motions, such that $dW_t dW_t{}' = \rho(X_t)dt$.

2.3   Historical Volatility in MMGBM

Volatility in the MMGBM model is modulated by a continuous time Markov chain. It changes when there is a regime change in the Markov chain, else it remains constant. This leads to the volatility to behave as a step function which is a pure jump process. However, with pure jump volatility one can observe diffusion type dynamics of historical volatility conventionally observed through data. A numerical approach is taken to establish the diffusion type dynamics of historical volatility by considering a pure jump volatility in an MMGBM model. The approach is as follows:

The stock price S_t, follows the MMGBM model. The estimator of historical volatility $\hat{\sigma}_t$ is calculated for an interval of $'d'$ days over a period of time T. The square of estimator volatility is called estimator of variance given by, $\hat{\sigma}^2$. The estimator of historical volatility is given by $\hat{\sigma}_t$. δ is the time step considered. Return of the stock $R_{t-\delta}$ is given by,

$$R_{t-\delta} = \frac{S_t - S_{t-\delta}}{S_{t-\delta}}, \tag{2.3.1}$$

where the stock price S_t, follows an MMGBM process.

$$\hat{V}(R_{t-\delta}) = \frac{\sum_{i=1}^{20} R_{t-i\delta}{}^2}{20} - \left(\frac{\sum_{i=1}^{20} R_{t-i\delta}}{20}\right)^2 \tag{2.3.2}$$

$$\hat{\sigma}_t^2 = \frac{\hat{V}(R_{t-\delta})}{\delta}, \text{ is the estimator of historical variance.} \tag{2.3.3}$$

In order to observe the diffusion type dynamics as well as the mean reverting nature of historical volatility

resulting from a pure jump volatility Monte Carlo simulations were run of the model (2.2.1) on MATLAB using the parameters given below :

1. Total time, T=3 (in years), Time step, δ=1/253 year

2. Initial stock price at time t=0, S_0=100.

3. 3 states: 1, 2, 3 are considered with, initial state $X_0 = 1$ and Rate Matrix, $\Lambda = \begin{bmatrix} -0.1 & 0.08 & 0.02 \\ 0.01 & -0.02 & 0.01 \\ 0.015 & 0.035 & -0.05 \end{bmatrix}$.

$\sigma(1) = 0.05$, $\sigma(2) = 0.10$, $\sigma(1) = 0.20$ and $\mu(1) = 0.02$, $\mu(1) = 0.08$, $\mu(1) = 0.04$.

Figure 2.1 is the simulation of as single realization of historical volatility over a 3 year period.
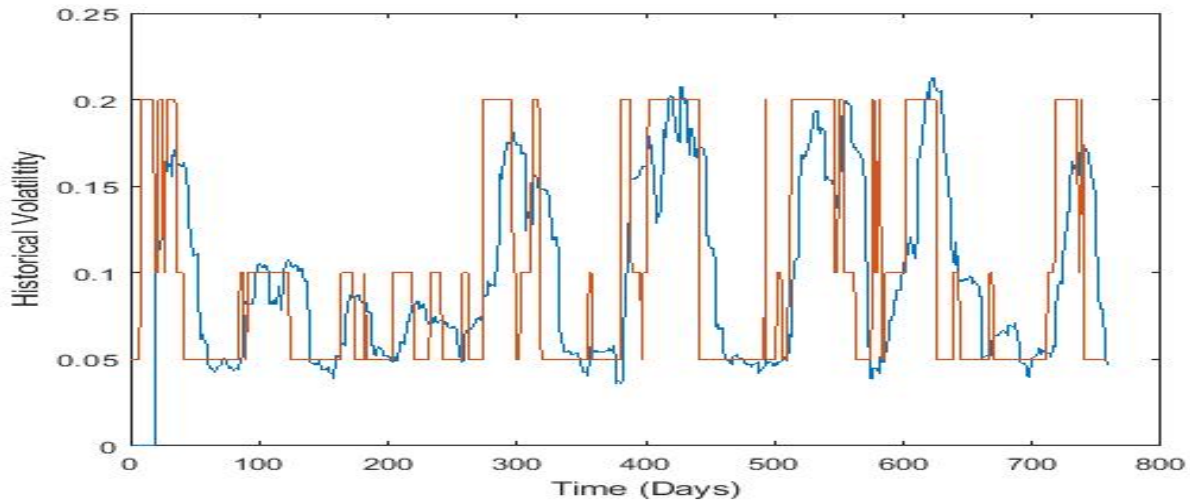
Figure 2.1: Single Realization of Historical Volatility

From the figure 2.1 the diffusion type dynamics of historical volatility can be observed. Another observation that can be made from the figures is the mean reverting nature of historical volatility. Mean reverting nature is displayed here as the the value of historical volatility rises and falls but tends to approach a mean value after each rise and fall. These numerical simulations and the following observations of diffusion type dynamics and mean reverting nature of the historical volatility process that is empirically observed in market data validates the claim of considering volatility to behave as a pure jump process.

Chapter 3

Inference of Jumps in Merton's Jump Diffusion model

In this chapter, we detail a statistical method for detection of jump discontinuities in the asset return data using a threshold approach. As the diffusion noise and the jump, both, contribute to the second order moment of the return process, the knowledge of return's variance alone is not sufficient to solve the calibration problem of both jump and diffusion coefficients. More insight(information) can be obtained from the classification of the returns using a threshold. In the standard threshold approach, to calibrate volatility, the annualized coefficient of diffusion term, the jump coefficients are inferred in advance. In this thesis we propose approach of maximal threshold where the jump detection and the volatility coefficients are obtained simultaneously. In our method for jump inference we consider a more generalized version of the original Merton's Jump Diffusion(MJD) model[49] where we relax the condition of jump sizes following a log-normal distribution.

3.1 Model Hypothesis

For detection of jump discontinuities, a simplified continuous-time model of asset price process, $S := \{S_t\}_{t \in [0,T]}$, is considered which is given by,

$$dS_t = \mu S_{t-} dt + \beta S_{t-} dW_t + S_{t-} dM_t \tag{3.1.1}$$

with $S_0 > 0$, where $W = \{W_t\}_{t \in [0,T]}$ is the standard Brownian motion, and $M = \{M_t\}_{t \in [0,T]}$ is a compound Poisson process. In particular, M is given by $M_t = \sum_{i=1}^{\mathcal{N}_t} \xi(i)$, in which $\mathcal{N} = \{\mathcal{N}_t\}_{t \in [0,T]}$ is a Poisson process with intensity Λ and $\xi := \{\xi(i)\}_{i=1,2,\ldots}$ is a sequence of independent random variables with identical cumulative distribution function (cdf) F having mean zero and a finite variance. We assume that W, $\mathcal{N}$ and ξ are independent to each other. It should be noted that (3.1.1) implies the following model

$$\frac{S(i) - S(i-1)}{S(i-1)} - \mu\Delta = \beta\sqrt{\Delta}Z(i) + (M_{i\Delta} - M_{(i-1)\Delta}) \tag{3.1.2}$$

for the discrete time series $(S(0), S(1), S(2), \ldots, S(N))$ having time step Δ (in year unit), where, $\{Z(i)\}$ are independent, identically distributed (i.i.d.) standard normal random variables. Here $S(i)$ stands for $S_{i\Delta}$ in (3.1.1). From a given equispaced data the one-step simple return is given by $r(i) = \frac{S(i) - S(i-1)}{S(i-1)}$. The average $\bar{r}$ of $\{r(1), \ldots, r(N)\}$ is given by $\bar{r} = \frac{1}{N} \sum_{i=1}^{N} r(i)$. Using (3.1.2) and the model assumption that $E\xi(i) = 0$, it is evident that $\bar{r}$ is an unbiased estimator of $\mu\Delta$. In addition, Our assumptions on F are:

(A1) $F(-1)$ is assumed to be zero,

(A2) $F(0-) = F(0)$, i.e., zero is a point of continuity of F.

Assumption (A1) ensures the positivity of S, while (A2) implies that $P(\xi = 0) = 0$. Specifically, (A2) prohibits jumps of size zero in simple return which does not impose any practical restriction on (3.1.1), but justifies selection of the CDF of jump size and the jump intensity. In the classical Merton's Jump Diffusion(MJD) model F is the CDF of one less than lognormal and hence MJD obeys (A1) and (A2). Even though (3.1.1) is of a more general nature than a classical MJD, (3.1.1) would be referred to as the MJD model hereon for the terminological convenience.

3.2   Motivation of Threshold Method

Empirical study by model fitting requires the estimation of all the parameters i.e. historical μ, β, Λ and F where, F is a functional parameter. The jump discontinuities, which are apparent in a continuous time process, but their identification becomes ambiguous when the process is observed in discrete time. In the following simple lemma it can be seen that the false positive error in jump detection can be reduced as the time step decreases.

Lemma 3.2.1. *Under no jump conditions and our assumptions: Given any $\hat{p} \in (0,1)$, and $c > 0$, there exists a sufficiently small $\Delta > 0$, such that $P(\bigcup_{i=1}^{N}\{|r(i) - \mu\Delta| \geq c\}) < \hat{p}$.*

Proof. Due to (3.1.2), under $\Lambda = 0$, $\{r(1), \ldots, r(N)\}$ is a sequence of i.i.d normal variables with mean $\mu\Delta$ and variance $\beta^2\Delta$. Let $A_i := \{\omega \in \Omega \mid |r(i) - \mu\Delta| \geq c\}$, then

$$P(A_i) = 2\left(1 - \Phi\left(\frac{c}{\beta\sqrt{\Delta}}\right)\right)$$

for each i, where Φ denotes the cdf of the standard normal distribution. Therefore,

$$P\left(\bigcup_{i=1}^{N} A_i\right) = 1 - P\left(\bigcap_{i=1}^{N}(\Omega \setminus A_i)\right) = 1 - \prod_{i=1}^{N}(1 - P(A_i)) = 1 - \left(2\Phi\left(\frac{c}{\beta\sqrt{\Delta}}\right) - 1\right)^N.$$

Hence the lemma is true, i.e., left side is less than $\hat{p}$ if and only if

$$2\Phi\left(\frac{c}{\beta\sqrt{\Delta}}\right) - 1 > (1 - \hat{p})^{1/N} = (1 - \hat{p})^{\frac{\Delta}{T}}$$

$$\text{or, } \frac{T}{\Delta} \ln\left(2\Phi\left(\frac{c}{\beta\sqrt{\Delta}}\right) - 1\right) > \ln(1 - \hat{p}) \tag{3.2.1}$$

where T denotes the length of the time horizon (i.e., $T = N\Delta$). A direct calculation gives that the left side of the above inequality vanishes as Δ goes to zero whereas right side is a fixed negative quantity. Hence there is a sufficiently small $\Delta > 0$ such that (3.2.1) is true. Hence the proof is completed. $\qquad\square$

Due to the continuity (see (A2)) of F at zero, given any $\hat{p} > 0$, there is a positive c such that for any $x \in (-c, c)$, one has $|F(x) - F(0)| < \hat{p}/2$. This gives

$$0 \leq F(c) - F(-c) < \hat{p}, \tag{3.2.2}$$

that is $P(|\xi| < c) < \hat{p}$. In other words, if such a value of c is set as threshold, the chance of false negative in jump detection becomes less than $\hat{p}$.

Remark 3.2.1. *Based on Lemma 3.2.1 and the implication (3.2.2) of (A2), the noise sources, i.e., Z (diffusion noise) and M (jump noise) in the discrete time series (sampled from (3.1.2)) can be separated with the help of an suitable threshold parameter c with confidence $1 - \hat{p}$, if the time discretization is sufficiently small. Therefore the value of c plays a crucial role in classification of noise. The estimation of c as in (3.2.2) is virtually impossible from a real data, computing a lower bound so that (3.2.1) holds for any value of c higher than that is practicable. Hence, a threshold obtained facilitates the false positive error to be bounded by $\hat{p}$. This is delineated further in this section.*

Definition 3.2.1. *Considering the above remark, if $\hat{\beta}$ is an estimator of β, then $\hat{c} := \gamma\hat{\beta}$ where*

$$\gamma := \sqrt{\Delta}\,\Phi^{-1}\left(\frac{1 + (1 - \hat{p})^{\frac{\Delta}{T}}}{2}\right), \tag{3.2.3}$$

is a known positive constant. Given a time series data, a jump is said to have occurred at i^{th} time step if $|r(i) - \bar{r}|$ is not less than $\hat{c}$ and at that instance, the value of the jump size is, $r(i) - \bar{r}$.

3.3 Maximal Threshold

An estimator (SD) of the standard deviation of one-step return is considered by [1]

$$SD^2 = \frac{1}{N}\sum_{i=1}^{N}\left(r(i) - \bar{r}\right)^2.$$

It should also be noted that SD^2 does not depend on $\hat{p}$. Following from, (3.1.2), an estimator $\hat{\beta}$ of β, can be chosen to follow

$$SD^2 = \hat{\beta}^2\Delta + \hat{\Lambda}\Delta V, \tag{3.3.1}$$

---

[1]It is a consistent estimator. In addition, as Δ is supposed to be chosen significantly small, let's say a few minutes in year unit. This leads to the magnitude of SD being small. In a typical time series data, conventionally, N is significantly large. Therefore, the bias in SD^2 is negligible.

where $\hat{\Lambda}$ and V are estimators of jump intensity and the variance of jump sizes. To observe this, it needs to be noted that, the variance formula of compound Poisson process, i.e., $VAR(M_t) = \Lambda t E(\xi^2)$. Let,

$$\hat{\Lambda} := \frac{card(I_{\hat{c}})}{T}, \tag{3.3.2}$$

where $I_{\hat{c}} = \{i \in \{1, \ldots, N\} \mid |r(i) - \bar{r}| \geq \hat{c}\}$ and $card(A)$ denotes the cardinality of a set A. Next, $\hat{\Lambda}$ is a plug-in estimator of Λ based on maximum likelihood estimation. Further, V as $V := \frac{\sum_{i \in I_{\hat{c}}} (r(i) - \bar{r})^2}{card(I_{\hat{c}})} = \frac{\sum_{i \in I_{\hat{c}}} (r(i) - \bar{r})^2}{\hat{\Lambda} T}$ (using (3.3.2)). Plugging in SD^2, V and $\hat{\Lambda}$ as above in (3.3.1), we get the following

$$G(\hat{\beta}) := \hat{\beta}^2 - \frac{SD^2}{\Delta} + \frac{1}{T} \sum_{i \in I_{\gamma\hat{\beta}}} (r(i) - \bar{r})^2 = 0. \tag{3.3.3}$$

$\hat{\Lambda} = \frac{card(I_{\gamma\hat{\beta}})}{T}$ and subsequently $V = \frac{\sum_{i \in I_{\gamma\hat{\beta}}} (r(i) - \bar{r})^2}{\hat{\Lambda} T}$ can be obtained from the solution of the above equation.

(3.3.3) evidently has a trivial solution $\hat{\beta} = 0$, which results in $\hat{\Lambda} = \frac{N}{T} = 1/\Delta$ and $V = SD^2$. In contrast we focus on the nontrivial solution where $\hat{\beta} > 0$, as higher the magnitude of $\hat{\beta}$ smaller the time points attributed to being jumps. In essence, we focus on the largest solution to (3.3.3), as our objective is to minimize the false-positive error in jump detection. A low false-positive error means the return series is explained by the diffusion term as much as possible.

Theorem 3.3.1. *The equation (3.3.3) has a non-trivial solution for sufficiently small $\hat{p}$.*

Proof. We need to prove the existence of a nontrivial zero of G (the function of $\hat{\beta}$ that is defined on the left side of (3.3.3)). It is evident that if $\hat{\beta}$ is more than $SD/\sqrt{\Delta}$, $G(\hat{\beta})$ is strictly positive. Hence any positive solution if exists lies in $(0, SD/\sqrt{\Delta}]$. Again, (3.2.3) implies that $\lim_{\hat{p} \to 0} \gamma = \infty$. Therefore,

$$\lim_{\hat{p} \to 0} \sum_{i \in I_{\gamma\hat{\beta}}} (r(i) - \bar{r})^2 = 0$$

as $I_{\gamma\hat{\beta}}$ becomes empty for a sufficiently large γ. Thus for any $\hat{\beta} \in (0, SD/\sqrt{\Delta})$, there is a sufficient small $\hat{p}$ such that $G(\hat{\beta})$ is strictly negative. We fix such $\hat{p}$. Since G is positive on $(\frac{SD}{\sqrt{\Delta}}, \infty)$, we conclude that G is bounded below and rises from negative to positive as $\hat{\beta}$ increases. This confirms existence of a zero of G if each discontinuity of G is due to a negative jump. Moreover, G, being bounded below, if additionally possesses right-continuity and has positive first order derivative at each point of continuity, would permit a minimizer $\hat{\beta}_{\min}$, say.

The above properties of G, can be established by considering the term $\frac{1}{T} \sum_{i \in I_{\gamma\hat{\beta}}} (r(i) - \bar{r})^2$, a non-increasing right continuous step function of $\hat{\beta}$. As G is the sum of this term with a continuous function $\hat{\beta}^2$ and a constant, G is also right continuous, having only negative jumps and a positive first and second order derivatives at the points of continuity. Hence, G has at least one zero on $(\hat{\beta}_{\min}, SD/\sqrt{\Delta})$. $\square$

Remark 3.3.1. *It is of crucial importance to take into account that (3.3.3) must be solved numerically for a given data set. Uniqueness of non-trivial zero is not obvious since G, is discontinuous. Since, G is strictly positive*
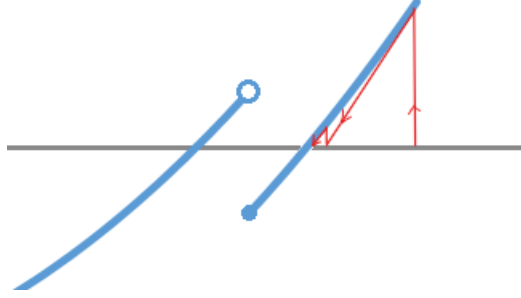
Figure 3.1: Convergence of gradient descent to the largest solution of (3.3.3)

beyond $SD/\sqrt{\Delta}$, there exists a finite largest zero of G which is strictly positive and unique, provided G becomes negative. This is also the desired solution to (3.3.3). It is to be observed that G is right continuous and also has a right derivative. Specifically, $G'(\beta) = 2\beta$, where G' is the right derivative of G. Therefore, the following Newton-Raphson algorithm with initial point $\frac{SD}{\sqrt{\Delta}}$ converges to the largest non-trivial solution(described above) rapidly

$$\beta_{n+1} = \beta_n - \frac{G(\beta_n)}{2\beta_n}, \quad \forall n \geq 0, \; and \quad \beta_0 = SD/\sqrt{\Delta}. \tag{3.3.4}$$

This is evident as G has jumps of negative size and has positive first and second order derivatives at the points of continuity and the initial point is on the right of the desired solution. It can be observed from Figure 3.1.

Definition 3.3.1 (Maximal Estimators)**.** *Let the limit of the iterative sequence* (3.3.4) *be defined as $\hat{\beta}_{\max}$ and term it as the* maximal estimator *of β parameter. Further more, the product $\gamma\hat{\beta}_{\max}$ is in fact defined as the maximal threshold and denote that by $\hat{c}_{\max}$.*

Evidently, the above mentioned threshold method is disparate to the standard method based on obtaining a fixed threshold. The approach in this thesis is termed as the maximal threshold method due the accuracy of jump-detection being optimized by controlling the false-positive error. We achieve this objective by obtaining the threshold and the volatility simultaneously by an iterative scheme. The theorem below with an independent theoretical interest, answers the question of uniqueness question of (3.3.3) on a restricted set. Furthermore, it also indicates the location of the estimator.

Theorem 3.3.2. *For a sufficiently small $\hat{p}$,* (3.3.3) *has a unique solution on $\left(\frac{SD}{\sqrt{2\Delta}}, \frac{SD}{\sqrt{\Delta}}\right]$ and no solution on $\left(\frac{SD}{\sqrt{\Delta}}, \infty\right)$.*

Proof. Let $\beta_0 = \frac{SD}{\sqrt{2\Delta}}$ and $\gamma_0 := \max_{i \leq N}\left(\frac{|r(i) - \bar{r}|}{\beta_0}\right)$. We fix $\hat{p}$ sufficiently small, so that γ in (3.2.3) is more than γ_0. Hence for all $\hat{\beta}$ not less than β_0, $\gamma\hat{\beta}$ is greater than $\max_{i \leq N}|r(i) - \bar{r}|$ and consequently $I_{\gamma\hat{\beta}}$ is empty. Therefore, at $\hat{\beta} = \beta_0$, G is equal to $-\beta_0{}^2$, a negative quantity; and continues to increase continuously on (β_0, ∞) and is positive at $\hat{\beta} = \frac{SD}{\sqrt{\Delta}}$. Hence the proof. $\square$

The computation $\hat{\beta}_{\max}$ has been elucidated so far, mainly to obtain a threshold value $\hat{c}_{\max}$. The threshold facilitates the isolation of the jumps from diffusion noise in return series with a confidence $1 - \hat{p}$. The class of data points

having jumps, can be analyzed alone for inferring the jump size distribution F. In addition, the return series which is driven or controlled by only diffusion can also be analyzed separately for the fitting other sophisticated diffusion models. This aspect is dealt in detail in the subsequent sections.

3.4 Consistency of $\hat{\beta}$

In this section the issues pertinent to the consistency of the estimator $\hat{\beta}$ as $\Delta \to 0$ are discussed. It can be observed that $\hat{\beta}$ depends on γ which in turn is dependent on both Δ and the choice of the mis-classification probability or probability of separation, $\hat{p}$. To enable $\hat{\beta}$ to only depend on Δ, the probability of mis-classification must be considered to be dependent on Δ and must approach zero as $\Delta \to 0$, rather than fixing a constant pre-assigned value $\hat{p}$. It is evident that the decay rate of the misclassification probability plays a key role in establishing consistency of the estimator. The missclassification probability is chosen as follows,

$$\hat{p} = \min\left(1, \alpha\Delta^{\ln(1/\Delta)}\right) \tag{3.4.1}$$

for some $\alpha > 0$. It can be seen that, $\hat{p} \to 0$ as $\Delta \to 0$. By choosing α carefully, a value of our choice can be assigned to $\hat{p}$. Hereon, we denote the right side of (3.2.3) as $\gamma(\Delta)$ in which $\hat{p}$ is defined as (3.4.1). By the following lemma, we prove that this choice of $\hat{p}$ gives a consistent estimator.

Lemma 3.4.1. *Let $\gamma(\Delta)$ be as above. Then as Δ tends to 0,*

1. *$\gamma(\Delta)$ converges to zero and*

2. *$\frac{\Delta \ln \frac{1}{\Delta}}{\gamma(\Delta)^2}$ converges to zero.*

Proof. It follows from the formula 7.1.13 of [34] that for any $x \geq 0$

$$\frac{1}{x + \sqrt{x^2 + 4}} < \sqrt{\frac{\pi}{2}} e^{\frac{x^2}{2}} (1 - \Phi(x)) < \frac{1}{x + \sqrt{x^2 + \frac{8}{\pi}}}. \tag{3.4.2}$$

Therefore for any $\varepsilon \geq 0$, we have that

$$\frac{e^{\varepsilon x^2}}{x + \sqrt{x^2 + 4}} < \sqrt{\frac{\pi}{2}} e^{x^2(\frac{1}{2} + \varepsilon)} (1 - \Phi(x)) < \frac{e^{\varepsilon x^2}}{x + \sqrt{x^2 + \frac{8}{\pi}}}. \tag{3.4.3}$$

Now substituting x by $\frac{x}{\sqrt{\frac{1}{2} + \varepsilon}}$ in the left hand side of the inequality (3.4.3), we deduce

$$e^{x^2}\left(1 - \Phi\left(\frac{x}{\sqrt{\frac{1}{2} + \varepsilon}}\right)\right) > \sqrt{\frac{2}{\pi}} \frac{\sqrt{\frac{1}{2} + \varepsilon} e^{\frac{\varepsilon}{\frac{1}{2} + \varepsilon} x^2}}{x + \sqrt{x^2 + 4\varepsilon + 2}}.$$

Since the right side diverges to infinity as $x \to \infty$, given any $M > 0$, there exists a $x_0 > 0$ such that for all $x \geq x_0$,

14

we have $1 - \Phi\left(x/\sqrt{\frac{1}{2} + \varepsilon}\right) > Me^{-x^2}$. Again, since Φ is non-decreasing, we obtain

$$x/\sqrt{\frac{1}{2} + \varepsilon} < \Phi^{-1}\left(1 - Me^{-x^2}\right). \tag{3.4.4}$$

On the other hand, substitution of x by $\sqrt{2}x$ in the right side of the inequality (3.4.2), gives convergence of $e^{x^2}\left(1 - \Phi\left(\sqrt{2}x\right)\right)$ to 0 as $x \to \infty$, in other words, given any $M > 0$, there exists a $x_0' > 0$ such that for all $x \geq x_0'$, we have the following

$$\sqrt{2}x > \Phi^{-1}\left(1 - Me^{-x^2}\right). \tag{3.4.5}$$

With slight abuse of notation, we denote $x_0 := \max\{x_0, x_0'\}$. Then (3.4.4) and (3.4.5) hold for any $x \geq x_0$. For a fixed $\hat{p} \in (0,1)$ and sufficiently large $x \geq x_0$, let $y > 0$, be such that the following holds

$$1 - Me^{-x^2} = \frac{1 + (1 - \hat{p})^y}{2}.$$

By using the Taylor's series expansion of $(1 - \hat{p})^y$, from above we obtain

$$x^2 = -\ln\left(\frac{\hat{p}y}{2M} + o(y)\right).$$

Then there is a $y_0 > 0$ such that for all $y < y_0$, we have

$$\sqrt{\ln\left(\frac{4M}{\hat{p}y}\right)} > x = \sqrt{-\ln\left(\frac{\hat{p}y}{2M} + o(y)\right)} > \sqrt{\ln\left(\frac{M}{\hat{p}y}\right)}. \tag{3.4.6}$$

Now by using (3.4.6) in (3.4.4), and by setting $y = \frac{\Delta}{T}$, for all $\Delta < \Delta_0$ with $\Delta_0 = Ty_0$, we deduce

$$\sqrt{\ln\left(\frac{MT}{\hat{p}\Delta}\right)} < \sqrt{\frac{1}{2} + \varepsilon}\,\Phi^{-1}\left(\frac{1 + (1 - \hat{p})^{\frac{\Delta}{T}}}{2}\right) = \left(\frac{1}{2} + \varepsilon\right)^{1/2}\frac{\gamma(\Delta)}{\sqrt{\Delta}},$$

provided $\hat{p} = \min\left(1, \alpha\Delta^{\ln(1/\Delta)}\right)$. Without loss of generality, assume Δ_0 sufficiently small so that $\hat{p} < 1$ for any $\Delta < \Delta_0$. By substituting $M = 1$ in the above inequality, and by squaring both sides we get

$$0 < \ln\left(\frac{T}{\alpha}\right) + \ln\left(\frac{1}{\Delta}^{\ln(1/\Delta)}\right) + \ln\left(\frac{1}{\Delta}\right) < \left(\frac{1}{2} + \varepsilon\right)\frac{\gamma^2(\Delta)}{\Delta}, \quad \forall\,\Delta < \Delta_0. \tag{3.4.7}$$

Or,

$$\frac{\Delta}{\gamma^2(\Delta)}\ln(T/\alpha) + \frac{\Delta}{\gamma^2(\Delta)}\left(\ln(1/\Delta)\right)^2 + \frac{\Delta}{\gamma^2(\Delta)}\ln(1/\Delta) < \left(\frac{1}{2} + \varepsilon\right).$$

Note that the second term of the left hand side of the above inequality is strictly dominating over the other terms as $\Delta \to 0$ and also the sum is bounded. This implies that the terms other than the second vanish as $\Delta \to 0$. Thus we prove our second claim, i.e., $\frac{\Delta \ln \frac{1}{\Delta}}{\gamma(\Delta)^2} \to 0$ as $\Delta \to 0$. Again, by using (3.4.6) in (3.4.5), and by setting $y = \frac{\Delta}{T}$, for

all $\Delta < \Delta_0$, we get that

$$\sqrt{\ln\left(\frac{4MT}{\hat{p}\Delta}\right)} > \sqrt{\frac{1}{2}}\frac{\gamma(\Delta)}{\sqrt{\Delta}}$$

provided $\hat{p} = \min\left(1, \alpha\Delta^{\ln(1/\Delta)}\right)$ where $\alpha > 0$. By substitute $M = 1$ and simplifying we obtain

$$2\Delta\left(\ln\left(\frac{4T}{\alpha}\right) + \ln(1/\Delta) + (\ln(1/\Delta))^2\right) > \gamma^2(\Delta),$$

for $\Delta < \Delta_0$. Hence the first claim is true as the left hand side of the above converges to 0 as $\Delta \to 0$. $\square$

Theorem 3.4.2. *Let β be the positive volatility parameter appearing in* (3.1.1) *and $\hat{\beta}_{\max}$ as in definition* 3.3.1. *As $\Delta \to 0$, $\hat{\beta}_{\max}$ converges to β in probability.*

Proof. Note that log return, i.e., the increment of log of asset price in Δ time span is

$$\ln(S_t) - \ln(S_{t-\Delta}) = \ln(S_t/S_{t-\Delta}) = \ln(1 + \frac{S_t - S_{t-\Delta}}{S_{t-\Delta}}). \tag{3.4.8}$$

On the other hand, $\frac{S_t - S_{t-\Delta}}{S_{t-\Delta}}$ is the simple return on the same time span and goes to zero as $\Delta \to 0$ provided t is not a jump time. Hence, using (3.4.8) and $\lim_{x\to 0}\frac{\ln(1+x)}{x} = 1$, we can write $\ln(S_t) - \ln(S_{t-\Delta}) \sim \frac{S_t - S_{t-\Delta}}{S_{t-\Delta}}$. Therefore, $\hat{c}_{\max}^2$, the threshold on the square of simple return also serves as the threshold on the square of log return as $\Delta \to 0$. Hence Corollary 2 in [43] gives that $\hat{\beta}_{\max} \to \beta$ in probability provided, $\hat{c}_{\max}^2$ and $\frac{\Delta\ln\frac{1}{\Delta}}{\hat{c}_{\max}^2}$ vanish as $\Delta \to 0$.

First note that, due to the finite activity jump, $SD^2 = O(\Delta)$ as $\Delta \to 0$. Thus by Theorem 3.3.2 we know that $\hat{\beta}_{\max}$ is bounded and away from zero provided $\beta \neq 0$. Therefore, $\hat{c}_{\max}^2$ and $\gamma^2(\Delta)$ share the same asymptotic. Finally the result follows from Lemma 3.4.1. $\square$

3.5 Numerical Experiments

This section the study of the finite sample performance of the estimator and threshold is detailed, presented in definition 3.3.1 by performing numerical experiments involving accuracy evaluation of jump detection for a given family of simulated data. Specifically, the accuracy measure is defined as,

$$\text{Accuracy} := \frac{\text{True Positive} + \text{True Negative}}{\text{True Positive} + \text{False Positive} + \text{True Negative} + \text{False Negative}}.$$

For performing simulations, Merton's jump-diffusion (MJD) model (3.1.1) is considered with various values of β and all other parameters are fixed to their typical values. The parameters, $\mu = 0.1$, $\Lambda = 100$ are fixed and F is the cdf of $Lognormal(-\frac{\delta^2}{2}, \delta^2) - 1$, with $\delta = 0.0055$. Each simulated time series data is of length 18000 and has a granularity $\Delta = 1/18000$. For every value of β, the average accuracy of 1000 simulations is illustrated by a plot and displayed in a table below, where, the performance of maximal threshold is compared and contrasted with a

few fixed thresholds. The fixed thresholds are chosen from the those suggested in Section 5 of [43].

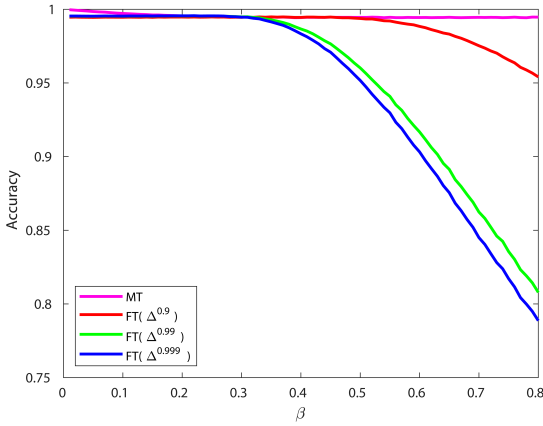| β	Using Maximal	Using Fixed Threshold		
values	Threshold	$\Delta^{0.9}$	$\Delta^{0.99}$	$\Delta^{0.999}$
0.01	0.9997	0.9946	0.9953	0.9954
0.1	0.9972	0.9946	0.9953	0.9954
0.2	0.9955	0.9947	0.9954	0.9955
0.3	0.9948	0.9947	0.9950	0.9948
0.4	0.9946	0.9947	0.9870	0.9838
0.5	0.9945	0.9938	0.9603	0.9517
0.6	0.9945	0.9885	0.9164	0.9027
0.7	0.9945	0.9755	0.8632	0.8459
0.8	0.9944	0.9541	0.8083	0.7887

Figure 3.2: Jump-detection Accuracy using Maximal threshold (MT) and Fixed threshold (FT) with values $\Delta^{0.9}$, $\Delta^{0.99}$ and $\Delta^{0.999}$.

Table 3.1: Mean accuracy of jump-detection using 1000 simulations of MJD model for different β and threshold values.

In Figure 3.2 the horizontal axis pertains to increasing values of the volatility parameter β and the vertical axis pertains to the accuracy measure in jump detection using a threshold method. Every line plot depicts the change of accuracy as β changes, corresponding to a particular threshold. We consider in addition to the maximal threshold, three different fixed thresholds, namely, $\Delta^{0.9}$, $\Delta^{0.99}$ and $\Delta^{0.999}$. Maximal thresholds are obtained by fixing $\hat{p} = 0.01$. A few numerical values are shown in Table 3.1.

It can be observed from Figure 3.2 and Table 3.1 that the accuracy measure reduces in the case of higher volatility when fixed threshold method for detecting jumps. In contrast we do not observe such a reduction in the case of Maximal threshold method.

In another numerical experiment the relative errors of the volatility estimators are obtained using four thresholds(Maximal and Fixed) as specified above. The analysis is conducted by varying β in $[0, 0.8]$ and considering six distinct δ values. Plots 1 to 6 in Figure 3.3 pertain to δ values of 0.0055, 0.01, 0.02, 0.03, 0.04, and 0.5 respectively. We can observe from the plots that the range of error is larger for larger δ which can be explained in the following manner. A large δ produces more jumps having smaller size which in turn causes higher number of false negative in jump detection when a fixed threshold is considered. In contrast, the linear dependence of maximal threshold on β, causes it to detect these small jumps if β is small. These typical small jumps are in fact, larger than the return size due to the diffusion noise given that, β is not very large. Therefore, the fixed threshold the estimation of small volatility is heavily affected by the presence a large number of outliers emanating from the small jumps which is the reason for the initial decline of relative error in small volatility estimation by fixed threshold when β increases. Plots 1 to 5 display an additional rise of error with β for higher β, occurring due to the increase of false positive in jump detection by the fixed thresholds. As maximal threshold grows linearly with β, the misclassifcation of large returns coming from diffusion noise as jumps does not occur.

17

Figure 3.3: Relative error vs true value in volatility estimation for $\delta = 0.0055$, 0.01, 0.02, 0.03, 0.04, and 0.5 respectively. The color legend of all six plots are identical to that of Figure 3.2.

The numerical experiments and explanations presented above justify the use of maximal threshold for jump detection. Therefore, maximal threshold method is used for the removal of jumps from the time series and consequently obtain the continuous part of the time series. The inference of the continuous part of the time series is presented in the subsequent sections.

Remark 3.5.1. *In [31], a Maximal threshold is obtained by minimizing Mean Square Error(MSE) in contrast to minimizing false positive error. Instead of MSE minimization if we obtain maximal threshold by minimizing false positive error, this later approach gives the threshold value immediately. In addition Minimization of false positive error produces Maximal threshold by straightforward arguments and the estimator of β is obtained simultaneously with the estimator of the threshold.*

3.6 Inference of Jumps in a Regime Switching Model

The Maximal threshold method discussed in the section 3.3 can be applied to models where volatility is not constant and varies, such as in a regime switching model and the consistency of estimators result from [43] will still hold. However, the motivation of the method of Maximal threshold would be lost as it mainly hinges on estimating a constant volatility parameter(based on the uni-regime Merton jump diffusion model), as the threshold is a function of the constant volatility parameter estimated. The calibrated constant volatility may not be meaningful in a stochastic volatility model such as a regime switching model.

Therefore, in this section only the accuracy of the maximal threshold would be compared with the fixed threshold

method in regime switching conditions. There would be no analysis on relative error of the estimated volatility parameter due to the above mentioned loss of meaning.

Numerical experiments involving accuracy evaluation of jump detection for a given family of simulated data of the regime switching Merton jump diffusion model with three regimes are performed.

For performing simulations, regime switching Merton's jump-diffusion (MJD) model (3.1.1) is considered with various values of $\beta = \bar{\sigma}$ and all other parameters are fixed to their typical values. The parameters corresponding to the three regimes i=1, 2, 3 are $\mu(1) = \mu(2) = \mu(3) = 0.07$, $\sigma(1) = \beta * (1 - \epsilon)$, $\sigma(2) = \beta$, $\sigma(3) = \beta * (1 + \epsilon)$, where $\epsilon = 0.8$, instantaneous transition rates, $\lambda_1 = 3000$, $\lambda_2 = 1000$, $\lambda = 2500$ and $\Lambda = 150$ are fixed and F is the cdf of Lognormal$(-\frac{\delta^2}{2}, \delta^2) - 1$, with $\delta = 0.0045$.

Each simulated time series data is of length 11000 and has a granularity $\Delta = 1/18000$. For every value of β, the average accuracy of 1000 simulations is illustrated by a plot and displayed in a table below, where, the performance of maximal threshold is compared and contrasted with a few fixed thresholds. The fixed thresholds are chosen from the those suggested in Section 5 of [43].

β	Using Maximal	Using Fixed Threshold		
values	Threshold	$\Delta^{0.9}$	$\Delta^{0.99}$	$\Delta^{0.999}$
0.01	0.9992	0.9946	0.9950	0.9951
0.1	0.9963	0.9946	0.9950	0.9951
0.2	0.9946	0.9946	0.9946	0.9945
0.3	0.9941	0.9942	0.9879	0.9864
0.4	0.9940	0.9914	0.9698	0.9649
0.5	0.9941	0.9848	0.9376	0.9286
0.6	0.9940	0.9725	0.8939	0.8813
0.7	0.9939	0.9545	0.8460	0.8307
0.8	0.9940	0.9309	0.7973	0.7805
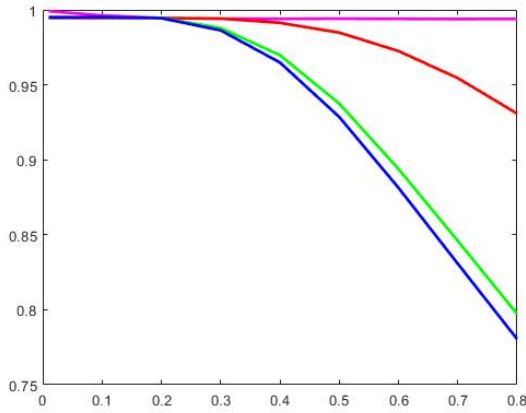
Figure 3.4: Jump-detection Accuracy in a regime switching model using Maximal threshold (MT) and Fixed threshold (FT) with values $\Delta^{0.9}$, $\Delta^{0.99}$ and $\Delta^{0.999}$.

Table 3.2: Mean accuracy of jump-detection using 1000 simulations of regime switching MJD model for different β and threshold values.

It can be observed from Figure 3.4(where X axis represents the β values and the Y axis represents the accuracy) and Table 3.2 that the accuracy measure reduces in the case of higher volatility when fixed threshold method for detecting jumps. In contrast we do not observe such a reduction in the case of Maximal threshold method. The maximal threshold method also has a higher accuracy than the fixed threshold methods for all volatility values considered.

Chapter 4

Squeeze-Expansion Based Inference of Regimes

4.1 Historical Volatility: Squeeze and Expansion Duration

From the knowledge of $\hat{\beta}$ obtained from the previous section, we have the threshold value $\hat{c} = \gamma\hat{\beta}$, for identifying the jump discontinuities. $\hat{\beta}$ and $\hat{c}$ denote $\hat{\beta}_{max}$ and $\hat{c}_{max}$ which implies that $\hat{c}$ is the maximal threshold value for identifying jump discontinuities.

For each $i = 1, \ldots, N$.

Define,

Definition 4.1.1. $\hat{r}(i) := \begin{cases} r(i) \text{ if } |r(i) - \bar{r}| \leq \hat{c} \\ \bar{r} \text{ else.} \end{cases}$

Hence $r(j) = \hat{r}(j) + (r(j) - \bar{r})\mathbb{1}_{[\hat{c},\infty)}(|r(j) - \bar{r}|)$. Thus, $\hat{r} = \{\hat{r}(i)|i = 1, \ N\}$ represents the simple return of the continuous part of the time series after removing the jump discontinuities. We use $\hat{r}$ to derive the historical volatility time series below.

Definition 4.1.2. $(\hat{\mu}, \hat{\sigma})$. *For a fixed window size n, the moving average $\{m(k)\}_{k=n}^{N}$ and the sample standard deviation $\{\sigma(k)\}_{k=n}^{N}$ are given by*

$$m(k) := \frac{1}{n}\sum_{i=0}^{n-1}\hat{r}(k-i),$$

$$\sigma(k) := \sqrt{\frac{1}{n-1}\sum_{i=0}^{n-1}(\hat{r}(k-i))^2 - \frac{n}{n-1}m(k)^2},$$

for $k \geq n$. The empirical volatility $\hat{\sigma} = \{\hat{\sigma}(k)\}_{k=n}^{N}$ is given by $\hat{\sigma}(k) := \dfrac{\sigma(k)}{\sqrt{\Delta}}$. The empirical drift $\hat{\mu} = \{\hat{\mu}(k)\}_{k=n}^{N}$ is

given by $\hat{\mu}(k) := \dfrac{m(k)}{\Delta}$.

Definition 4.1.3. *Let* $y = \{y_k\}_{k=1}^m$ *be a collection of random samples of a real valued random distribution. Then the empirical cumulative distribution function or ecdf* $\hat{F}_y$ *is defined as:* $\hat{F}_y(x) := \frac{1}{m}\sum_{k=1}^m 1_{[0,\infty)}(x - y_k)$ *where given a subset* $A, 1_A$ *denotes the indicator function of* A.

Definition 4.1.4. *(p-percentile). Let* $\hat{F}_y(p)$ *be the ecdf of* $y = \{y_k\}_{k=1}^m$. *Then for any* $p \in (0,1)$, *the p-percentile of* y, *denoted by* $\hat{F}_y^{\leftarrow}(p)$, *is defined as*

$$\hat{F}_y^{\leftarrow}(p) := \inf\{x | \hat{F}_y(x) \geq p\}.$$

Lemma 4.1.1. *Given a time series* $y = \{y_k\}_{k=1}^m$ *and* $p \in (0,1)$,

(i) $-\hat{F}_{-y}^{\leftarrow} = \hat{F}_y^{\leftarrow}(1 - p+),$

(ii) *and if* $p \in (0,1)\backslash\hat{F}_y(\mathbb{R})$, *then* $-\hat{F}_{-y}^{\leftarrow}(p) = \hat{F}_y^{\leftarrow}(1 - p),$

Proof. Let $x = -\hat{F}_{-y}^{\leftarrow}(p)$ say or $-x = \hat{F}_{-y}^{\leftarrow}(p)$. Hence using using definition of $\hat{F}$,

$$\hat{F}_{-y}\left(-x - \varepsilon\right) < p \leq \hat{F}_{-y}(-x) \,\forall \varepsilon > 0$$

$$\text{or, } \frac{card\{k| - y(k) \leq -x - \varepsilon\}}{N} < p \leq \frac{card\{k| - y(k) \leq -x\}}{N} \forall \varepsilon > 0$$

$$\text{or, } \frac{card\{k|y(k) \geq x + \varepsilon\}}{N} < p \leq \frac{card\{k|y(k) \geq x\}}{N} \forall \varepsilon > 0$$

$$\text{or, } 1 - \frac{card\{k|y(k) < x + \varepsilon\}}{N} < p \leq 1 - \frac{card\{k|y(k) < x\}}{N} \forall \varepsilon > 0$$

$$\text{or, } \frac{card\{k|y(k) < x + \varepsilon\}}{N} > 1 - p \geq \frac{card\{k|y(k) < x\}}{N} \forall \varepsilon > 0$$

$$\text{or, } \frac{card\{k|y(k) < x\}}{N} \leq 1 - p < \frac{card\{k|y(k) < x + \varepsilon\}}{N} \forall \varepsilon > 0$$

$$\text{or, } \frac{card\{k|y(k) \leq x - \varepsilon\}}{N} \leq 1 - p < \frac{card\{k|y(k) \leq x + \varepsilon\}}{N} \forall \varepsilon > 0$$

$$\text{or, } \hat{F}_y(x - \varepsilon) \leq 1 - p < \hat{F}_y(x + \varepsilon) \forall \varepsilon > 0$$

$$\text{or, } \hat{F}_y(x-) \leq 1 - p < \hat{F}_y(x)$$

since $\hat{F}_y$ is a right continuous step function. Hence, $x = \lim_{\varepsilon \to 0} \hat{F}_y^{\leftarrow}(1 - p + \varepsilon)$. Thus (i) is true.

If p is not in the range of $\hat{F}_y, p$ is strictly less than $\hat{F}_{-y}(-x)$. Then, $\hat{F}_y(x-) < 1 - p < \hat{F}_y(x)$, i.e., $x = \hat{F}_y^{\leftarrow}(1 - p)$. From Lemma (4.1.1), the range of $\hat{F}_y$, i.e., $\hat{F}_y(\mathbb{R})$ is $\{i/m | i = 0, 1, \quad m\}$ since $y = \{y_k\}_{k=1}^m$. Therefore $(0,1)\backslash\hat{F}_y(\mathbb{R}) = \bigcup_{i=1}^m (\frac{i-1}{m}, \frac{i}{m})$. By considering a particular p, the $100p$ percentile of $\hat{\sigma}$'would be used as the threshold in identifying the squeeze of the Bollinger band of return series. The definition of squeeze is presented below. $\qquad\square$

Definition 4.1.5. *(p-squeeze). Given a $p \in (0,1)$, an asset is said to be in p-squeeze at k-th time step if the empirical volatility $\hat{\sigma}(k)$, as defined above, is not more than $\hat{F}_{\hat{\sigma}}^{\leftarrow}(p)$.*

The definition of sojourn times of the p-squeeze is given below:

Definition 4.1.6. *By following the convention of $\min \varnothing = +\infty$, for a fixed $p \in (0,1)$ and a given time series $\{\hat{\sigma}\}_{k=n}^{N}$, let $\{(a_i,\ b_i)\}_{i=1}^{\infty}$ be an extended real valued double sequence given by*

$$\begin{cases} a_0 = n \\ b_{i-1} := \min\{k \geq a_{i-1}|\hat{\sigma}(k) > \hat{F}_{\hat{\sigma}}^{\leftarrow}(p) \\ a_i := \min\{k \geq b_{i-1}|\hat{\sigma}(k) \leq \hat{F}_{\hat{\sigma}}^{\leftarrow}(p), \end{cases}$$

for $i = 1,2,\ldots$. Then the collection of sojourn time durations for the p-squeezes is $d(\hat{\sigma};p) := \{d_i\}_{i=1}^{L}$, where $d_i := b_i - a_i$ and $L := \max\{i|b_i < \infty\}$, provided $L \geq 1$. d_i is the i-th entry of $d(\hat{\sigma};p)$ and L is the length of $d(\hat{\sigma};p)$.

d_i should be multiplied by Δ to obtain the squeeze duration in year unit. An application of Lemma (4.1.1) implies that $d(-\hat{\sigma};p)$ is the collection of sojourn time duration for p-expansions, i.e., the duration when $\hat{\sigma}(k) \geq \hat{F}_{\hat{\sigma}}^{\leftarrow}(1-p)$, provided p is not in the range of $\hat{F}_{\hat{\sigma}}$. To observe this one must note that if $d(-\hat{\sigma};p) = \{d_i\}_{i=1}^{L}$, then $d_i = b_i - a_i$, where $a_i = \min\{k \geq b_{i-1}| - \hat{\sigma}(k) \leq \hat{F}_{-\hat{\sigma}}^{\leftarrow}(p)\}$ which is same as $\min\{k \geq b_{i-1}|\hat{\sigma}(k) \geq \hat{F}_{\hat{\sigma}}^{\leftarrow}(1-p)\}$ and $b_{i-1} = \min\{k \geq a_{i-1}| - \hat{\sigma}(k) > \hat{F}_{-\hat{\sigma}}^{\leftarrow}(p)\} = \min\{k \geq a_{i-1}|\hat{\sigma}(k) < \hat{F}_{\hat{\sigma}}^{\leftarrow}(1-p)\}$ for $i \geq 1$ and $a_0 = n$. $d(\pm\hat{\sigma};p)$ is used to denote either $d(\hat{\sigma};p)$ or $d(-\hat{\sigma};p)$.

Remark 4.1.1. *(i) From the construction of $d(\pm\hat{\sigma};p)$ it can clearly be seen that $d(+\hat{\sigma};p)$ captures the duration of visiting low volatility, $d(-\hat{\sigma};p)$ captures that of visiting high volatility when p is smaller than half. When combined together, they would be able to capture the three regime scenario, namely, low, medium and high volatility switching dynamics if p is considerably smaller than half. After removing the jump term from model 3.1.1, one obtains a geometric Brownian motion which is also known as the BlackScholes-Merton model. To test the model hypothesis of a three regime switching Model, both $d(\hat{\sigma};p)$ and $d(-\hat{\sigma};p)$ would be considered together.*

4.2 A Discriminating Statistics

The asset price data of long time in the past has little use or relevance in modelling the price dynamics in more recent times. This necessitates an upper bar/limit on the length of the time series under consideration for inference purposes. This implies that for a time series data to be used for practical/empirical purposes, the length of $d(\pm\hat{\sigma};p)$ is considerably small. Let, $d = d(\pm\hat{\sigma};p)$ and $L = $ length of d. Hence, a non parametric estimation of the entries of d by the use of empirical cdf is not practicable as it would lead to a high standard error. Therefore, only a collection of few descriptive statistics like mean ($\bar{d}$), standard deviation(s), skewness(ν), kurtosis(κ) of d should be considered as they can be estimated reliably. Theoretically d is a random sequence with random length, the corresponding descriptive statistics constitute a random vector of fixed length. The sampling distribution of this vector is compared with the vector ($\bar{d}$, s, ν, κ) of the time series data to test the model hypothesis. For this purpose a discriminating statistics $T = (T_1,\ T_2,\ldots,T_r)$ is constructed using the first r number of descriptive statistics of d as follows:

$$T_1 := \frac{1}{L} \sum_{i=1}^{L} d_i,$$

$$T_2 := \sqrt{\frac{1}{L-1} \sum_{i=1}^{L} (d_i - T_1)^2},$$

$$T_3 := \frac{\frac{1}{L} \sum_{i=1}^{L} (d_i - T_1)^3}{T_2{}^3}$$

$$T_4 := \frac{\frac{1}{L} \sum_{i=1}^{L} (d_i - T_1)^4}{T_2{}^4}$$

and so on for the other numbers up to r.

The test statistics constitute durations which are in turn are correlated to the sojourn times of regime transitions, but it is not directly observable that, these statistics would capture the unobserved switching efficiently because of the randomness present in the Brownian motion. The effect of this randomness can be mitigated by considering a longer moving window size (n) for defining $\hat{\sigma}$ in definition (4.1.2). Unfortunately, a larger window size ignores a larger number of intermittent transitions often, which enhances the inaccuracy. Therefore $n = 20$ is fixed from hereon in the definition, which is the popular choice by practitioners for computing the empirical volatility.

Note: T^+ pertains to squeeze durations while T^- pertains to expansion durations and T is a generalised definition pertaining to both T^+ and T^-.

4.2.1 Rejection criteria based on the statistics

In this subsection the numerical computation of sampling distribution of T statistics is detailed under each model of the composite null hypothesis using Monte-Carlo simulation method, which is popularly known as typical surrogate approach following [47](see [48] for *composite hypothesis*). The rejection criterion is as follows:

(a) A non-empty subclass $\mathcal{A}$ of Θ, the class of models obeying the null hypothesis is fixed.

(b) For each $\theta \in \mathcal{A}, B$ number of time series $\{X^1, X^2, \ldots, X^B\}$ are sampled from the corresponding model θ with the same time step size present in S.

(c) Based on whether the discriminating statistics depend or pertain to squeeze or expansion, $d(\hat{\sigma}; p)$ or $d(-\hat{\sigma}; p)$ is considered respectively for defining T (T^+ or T^-) . For the class $\mathcal{A}$, then d is considered for defining T. Let $t^* := T(S)$ be the value of T of the observed data S and $t^* = (t_1^*, t_2^*, \ldots, t_r^*)$. Let $t^i = (t_1^i, t_2^i, \ldots, t_r^i) := T(X^i)$ for each $i = 1, \ldots, B$. Then t_θ denotes $\{t^1, t^2, \ldots, t^B\}$, the set of values of T for $\{X^1, X^2, \ldots, X^B\}$ corresponding to each $\theta \in \mathcal{A}$.

(d) In order to measure the proximity of t* with respect to the set t_θ, we define $g_B : \mathbb{R} \to [0, 1/2]$ given by $g_B(x) := \max(\dfrac{\min(x, (B-x))}{B}, 0)$ and a proximity measure,

$$\alpha_r^\theta := \min_{j \leq r} g_B(\sum_{i=1}^{B} 1_{[0,\infty)}(t_j^* - t_j^i)).$$

(e) The measure of proximity of the data to a class $\mathcal{A}$ is defined as, $\alpha_r = \max_{\theta \in \mathcal{A}} \alpha_r^\theta$.

(f) The hypothesis that S is a sample from a model in the class $\mathcal{A}$ can be rejected provided α_r is smaller than a predetermined value.

(g) The discriminating statistics are calculated pertaining to both squeeze and expansion durations as we do not know which of them is better sensitive to the data.

(h) Let r be the maximum of all i for which α_i is obtained. α_r^+ (pertaining to squeeze i.e T^+) and α_r^- (pertaining to expansion i.e. T^-) are calculated and the final proximity measure is obtained as follows:
$\alpha_r = \max(\alpha_r^+, \ \alpha_r^-)$
The set of parameters for the optimal or best fit model i.e. having the highest proximity measure is obtained as follows:
$\theta^* = \mathrm{argmax}_\theta(\alpha_r^+, \ \alpha_r^-)$.
The set of parameters θ^* is the model that has the highest proximity measure/ the maximized/optimal/best fit model and would be used further for simulations.

Note:We consider our discriminating statistic as $\alpha_r = \max(\alpha_r^+, \ \alpha_r^-)$, since, we do not know whether T^+ or T^- is more sensitive.

Remark 4.2.1. *It is to be noted that the above mentioned rejection has an empirical confidence level $100(1 - \alpha_r)$ when $r = 1$, i.e., the statistics is of a single dimension. On the other hand this expression is completely different from confidence level when the dimensions of statistics is large. This phenomenon is called the "curse of dimensionality". For a given model, the probability of observing the value of r to be smaller than a predetermined small value is not so small when r is considerably large.*

4.3 Discretization of Continuous Time Models

For testing of model hypothesis we a discrete time version of the continuous time theoretical asset price model given by,

$$dS_t = \mu(X_{t-})S_{t-}dt + \sigma(X_{t-})S_{t-}dW_t + S_{t-}dM_t, \tag{4.3.1}$$

for $t > 0$ with $S_0 > 0$, where $\{X_t\}_{t \geq 0}$ is a three state non explosive three state pure jump process.

Definition 4.3.1. *In this work, $\{X_t\}_{t \geq 0}$ is defined as a continuous three-state continuous Markov chain, with states defined as 1 , 2 and 3 respectively. This process does not permit the transition directly from state 1 to state 3 or vice versa without transitioning through state 2.*

Firstly, the Merton's Jump Diffusion (MJD) model which is uni-regime is considered. Two different composite model hypotheses, namely, (i)uni-regime MJD, (ii) Markov switching Ternary regime MJD, are considered in this work. The core objective of testing each such composite model hypothesis, is the simulation of the discrete version of continuous-time models selected from an appropriately chosen range of models satisfying the model assumption. An approximate procedure of identifying an appropriate class of reduced dimensions for a given data corresponding to each composite hypothesis is detailed in the following section.

As the test statistics T is computed after removing the jump discontinuities, it depends on only the continuous part of the data. Therefore for the purpose of inference, it is sufficient to simulate only the continuous part of the models. It is enough to simulate the following SDE (Stochastic Differential Equation) rather than the continuous version for comparing the sampling distribution of T

$$dS_t = S_t(\mu(X_t)dt + \sigma(X_t)dW_t), \tag{4.3.2}$$

where, $\{X_t\}_{t \geq 0}$ is a continuous three-state Markov process as in definition 4.3.1 and $\mu(X_t)$, $\sigma(X_t)$ are the drift and the volatility coefficients. Let $\{0 = t_0 < t_1 < \cdots < t_N\}$ be an equispaced partition of the time interval where $t_{i+1} - t_i = \Delta$ for $i = 0, 1, \ldots, N - 1$ and Δ is the length of time step in year unit and same as the granularity of the empirical data. We use this convention throughout this paper.

4.3.1 Uni-regime

In this subsection we consider the model hypothesis (3.1.1) for some arbitrary model parameters μ, β, Λ and F. After removing the jump term, the model reduces to

$$dS_t = S_t(\mu dt + \beta dW_t)t > 0, \ S_0 > 0. \tag{4.3.3}$$

Equation 4.3.3 has a strong solution of the form

$$S_t = S_0 \exp(\mu t - \frac{1}{2}\beta^2 t + \beta W_t) \ t \geq 0. \tag{4.3.4}$$

The discretized version of 4.3.4 is given by,

$$S_{t_0} = S_0, \ S_{t_{i+1}} = S_{t_i} \exp((\overline{\overline{\mu}} - \frac{1}{2}\overline{\overline{\sigma}}^2)\Delta + \overline{\overline{\sigma}}Z_i) \text{ for, } i = 0, 1, \ldots, N - 1 \tag{4.3.5}$$

where $\{Z_i | i = 0, \quad N - 1\}$ are independent and identically distributed (i.i.d) normal random variables with mean 0 and variance Δ.

4.3.2   Ternary Markov regime

Omission of the jump term from (4.3.1)reduces the model to (4.3.2) where X denotes a Markov chain as defined in 4.3.1.

As the continuous time Markov chain is characterized by its instantaneous transition rate matrix λ, the class of all possible models in (4.3.2) are identified with the set Θ of all possible parameters as given below,

$$\Theta = \{\theta = (\mu(1), \lambda_1, \lambda_{12}, \lambda_{13}, \sigma(1), \mu(2), \lambda_2, \lambda_{21}, \lambda_{23}, \sigma(2), \mu(3), \lambda_3, \lambda_{31}, \lambda_{32})|\mu(i) > 0, \lambda_i > 0, i = 1, 2, 3\}, \quad (4.3.6)$$

Using the expression of strong solution, the discrete version of models corresponding to each member of Θ can be written. However, we write down the discretization only for a smaller class of models which are relevant for the empirical study in the subsequent section. The scheme for X given below is the discretization of a Markov chain and the details can be found in theorem 5.3.1 in the next chapter.

$$S_{t_{i+1}} = S_{t_i} \exp((\mu(X_i) - \tfrac{1}{2}\sigma^2(X_i))\Delta + \sigma(X_i)Z_i), \quad (4.3.7)$$

$$X_{i+1} = X_i + ((2 - X_i) + (-\delta_{2,X_i})^{\eta_i})P_i \quad (4.3.8)$$

where, P_i and η_i are sequences of Bernoulli random variables, $\delta_{x,y}$ is the Kronecker delta function and 0^0 is taken as 0. Furthermore, η_i are iid and are independent of the past or present states of the Markov chain X_i. We also assume the following properties of $\{P_i\}$. The sequence $\{P_i|i = 1, \ldots, N-1\}$ are independent to Z_j for all j. For each given X_i, the conditional distribution of P_i is independent of $\{P_1, P_2, \ldots, P_{i-1}\}$ and η_i. For each i, P_i follows *Bernoulli* $(\lambda_{X_i}\Delta)$, a Bernoulli random variable with *Prob* $(P_i = 1|X_i) = \lambda_{X_i}\Delta$, provided $\Delta \ll \min\{1/\lambda_i|i = 1, 2, 3\}$. Here for each i, Z_i where $\{Z_i|i = 0, \ldots, N-1\}$ are independent and identically distributed (i.i.d) normal random variables with mean 0 and variance Δ.

Chapter 5

Empirical Study

5.1 Analysis of Market Data

The time series data of eighteen different Indian stock indices with 5-minute granularity during the time period starting from 1-st December, 2016 to 30-th June, 2017 are considered. We assume six hours of trading in each day and two hundred and fifty trading days in a year and set $\Delta = \dfrac{5}{250 \times 360} \approx 5.5 \times 10^{-5}$. For obtaining the jump discontinuities separately, we consider $\hat{p} = 1\%$ (by 3.4.1 $\hat{p} = \min\left(1, \alpha\Delta^{\ln(1/\Delta)}\right)$ and we choose $\alpha = 4.93 * 10^{39}$). Then (3.3.3) is solved numerically as it is described in remark 3.3.1.

The numerical approximations of $\hat{\beta}$, $\hat{\Lambda}$ and V for each index data are given in Table 5.1. Each row of Table 5.1 corresponds to an index, whose name is given in the second column with the code in the first column. By making use of the $\hat{\beta}$ value, the $\hat{c}$ value is obtained for each index using (4.1.2). Next, by using the value of $\hat{c}$, $\hat{\mu}$ and $\hat{\sigma}$ are computed based on the definition 4.1.2. In the last two columns of Table 5.1 the empirical long run average drift $\overline{\hat{\mu}}$ and the empirical long run average volatility $\overline{\hat{\sigma}}$ are displayed for each index.

Table 5.1: Estimated parameters of 5-min (1/12/16 - 30/06/17) data of 17 Indian stock indices

Index		$\hat{\beta}$	$\hat{\Lambda}$	V	$\bar{\hat{\mu}}$	$\bar{\hat{\sigma}}$
Code	Name	(in %)		(in 10^{-5})	(in %)	(in %)
I01	NIFTY 100	7.41	132.14	2	6.5	6.90
I02	NIFTY 200	7.54	127.36	2	8.7	7.00
I03	NIFTY 50	7.34	132.19	2	7.7	6.88
I04	NIFTY 500	7.62	143.43	2	10.5	6.70
I05	NIFTY BANK	10.39	128.90	5	24.8	9.75
I06	NIFTY COMMODITY	10.22	116.08	3	-4.8	9.47
I07	NIFTY ENERGY	10.93	148.24	4	-13.1	10.22
I08	NIFTY FIN. SER.	9.78	132.20	5	23.3	9.14
I09	NIFTY FMCG	11.89	167.58	5	17.7	11.04
I10	NIFTY INFRA	10.76	103.18	3	12.1	10.02
I11	NIFTY IT	11.26	157.88	4	5.5	10.33
I12	NIFTY MEDIA	14.64	120.90	6	13.9	13.64
I13	NIFTY METAL	16.24	99.95	6	-20.8	15.12
I14	NIFTY MNC	9.36	77.34	3	20.3	8.68
I15	NIFTY PHARMA	12.02	154.69	5	-26.2	11.07
I16	NIFTY PSE	10.25	148.32	3	-9.9	9.47
I17	NIFTY SERVICE SEC.	8.36	149.93	3	17.5	7.84

We recall that the 'T' test statistics described in section 4.2 are defined using $d(\pm\hat{\sigma}; p)$. In this section we fix $p = 15\%$ in the definition of the sub class of models $\mathcal{C}$ and obtaining $d(\pm\hat{\sigma}; p)$ and subsequently the T statistics . The t^* values are computed using $d(\hat{\sigma}; p)$ and $d(-\hat{\sigma}; p)$ separately. The components of t^* for every index data are given in Table 5.2.

Table 5.2: $\mathbf{t}^*$ of the empirical data

Index	Squeeze duration $d(\hat{\sigma}; p)$					Expansion duration $d(-\hat{\sigma}; p)$				
	L	t_1^*	t_2^*	t_3^*	t_4^*	L	t_1^*	t_2^*	t_3^*	t_4^*
I01	157	10.66	11.31	1.16	3.36	142	11.78	10.66	1.06	3.79
I02	169	9.89	11.12	1.34	3.92	142	11.76	10.48	0.94	3.32
I03	158	10.58	10.89	1.08	3.24	149	11.22	10.49	1.08	3.80
I04	157	10.65	11.24	1.21	3.60	142	11.76	10.29	0.90	3.37
I05	158	10.59	11.69	1.37	3.98	128	13.07	9.97	0.54	3.14
I06	168	9.95	10.55	1.47	4.57	136	12.29	10.03	0.83	3.59
I07	165	10.14	11.29	1.56	4.75	141	11.86	9.21	0.60	3.24
I08	172	9.72	10.85	1.54	4.61	124	13.48	10.40	0.82	3.72
I09	179	9.35	10.18	1.57	4.95	137	12.20	10.27	0.77	3.27
I10	176	9.50	11.69	1.73	5.43	128	13.06	11.71	1.27	5.09
I11	159	10.52	11.37	1.18	3.31	129	13.06	10.11	1.32	6.76
I12	174	9.61	9.50	1.21	3.86	120	12.97	10.79	0.60	2.82
I13	187	8.94	10.58	1.90	6.42	121	13.68	9.51	0.36	2.35
I14	178	9.40	10.64	1.53	4.62	127	13.12	9.99	0.60	3.26
I15	174	9.61	11.21	1.54	4.51	125	13.39	11.91	1.67	8.29
I16	148	11.30	12.66	1.28	3.75	140	11.94	10.69	0.98	3.54
I17	172	9.72	11.09	1.33	3.79	125	13.38	10.05	0.59	3.21

Remark 5.1.1. *As the hypothesis, we consider, is composite in nature(see [48] for composite hypothesis). That is to say the value of any parameter is not deemed to be fixed in the null hypothesis, which in turn leads to the consideration of models with parameters from a high dimensional space. Therefore, to reduce dimensions, we add some other natural criteria on parameters. These natural criteria desirably put direct and easily calculable constraints on the parameter set of the models under consideration.*

5.2 Uni-regime Model

In this subsection we consider the model hypothesis 3.1.1 of uni-regime Merton Jump Diffusion(MJD) model

Definition 5.2.1. *For simulation purposes we consider the sub-class of uni-regime MJD models with a unique choice of μ and β such that $\mu = \overline{\hat{\mu}}$ and $\beta = \overline{\hat{\sigma}}$, as used in definition 4.1.2 where the bar sign represents the time average.*

For each index in Table 5.1 and 5.2, we set our null hypothesis,

H_0 : the time series is in class of uni-regime MJD models in subclass defined in 5.2.1

The following figures illustrate the results for all 17 indices. Figure 5.1 displays the sampling distribution of T_1 of $d(\hat{\sigma}; p)$ and 5.2 illustrates that of $d(-\hat{\sigma}; p)$. Each box plot is obtained by simulating (4.3.5), 100 times. The

29

inverted triangle plots represent t_1^* obtained from the Table 5.2. As the dots appear to be non-overlapping with the box plots, the null hypothesis is rejected with 100% confidence.
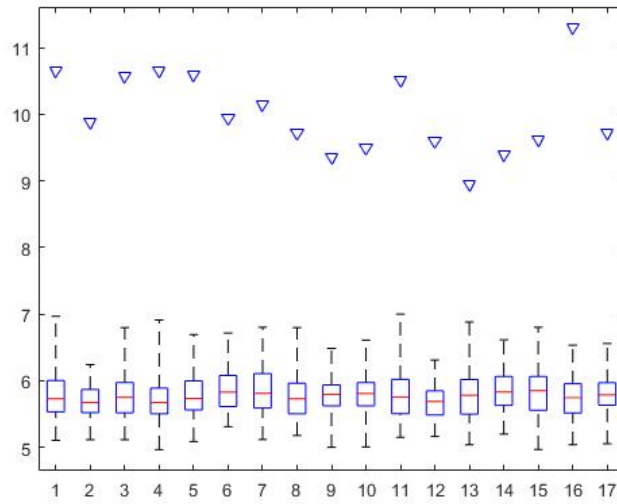

Figure 5.1: Sampling distribution of T1 of $d(\hat{\sigma}; p)$ under uni-regime MJD hypothesis
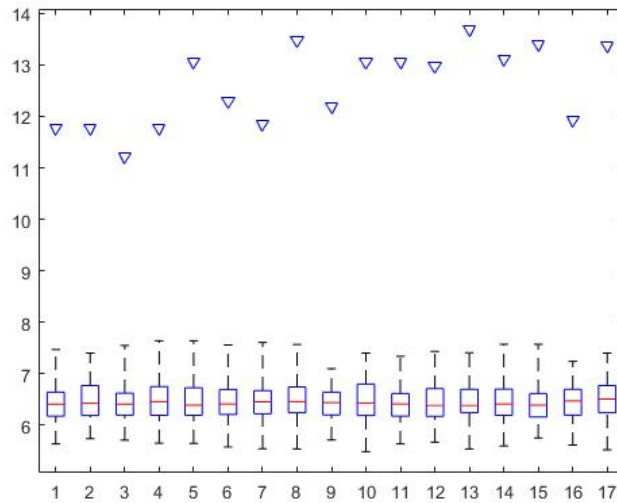
Figure 5.2: Sampling distribution of T1 of $d(-\hat{\sigma}; p)$ under uni-regime MJD hypothesis

5.3   Ternary regime Markov Model

This subsection details the sub class $\mathcal{C}$ of Ternary Regime Markov switching Merton Jump Diffusion (TRMJD) models defined in (4.3.2), which we consider for inference purposes. The subclass $\mathcal{C}$ is considered for reduction of dimensions and ease of computation. The same sub class models are considered for hypothesis testing.

In the following models in subclass $\mathcal{C}$, regime 1 is the low volatility regime, regime two is the medium volatility regime and regime 3 the high volatility regime. The continuous Markov chain X can be completely defined by its instantaneous transition rate matrix:

$$\Lambda = \begin{bmatrix} \lambda_{11} & \lambda_{12} & \lambda_{13} \\ \lambda_{21} & \lambda_{22} & \lambda_{23} \\ \lambda_{31} & \lambda_{32} & \lambda_{33} \end{bmatrix} . \lambda_{ii} = -\sum_{j \neq i} \lambda ij, \quad \text{where, } \lambda_i = -\lambda_{ii}, \text{for} i = 1, 2, 3. \tag{5.3.1}$$

The general class of models can be identified with the set of parameters Θ. Where,

$$\Theta = \{\theta = (\mu(1), \lambda_1, \lambda_{12}, \lambda_{13}, \sigma(1), \mu(2), \lambda_2, \lambda_{21}, \lambda_{23}, \sigma(2), \mu(3), \lambda_3, \lambda_{31}, \lambda_{32}) | \mu(i) > 0, \lambda_i > 0, i = 1, 2, 3\}. \tag{5.3.2}$$

As it is evident from (5.3.2) the general class of models are very high dimensional. For reducing the dimensionality and for computational feasibility, we consider a smaller subset of the general class of the models for inference purpose.

The sub class $\mathcal{C}$ of Ternary regime Markov/TRMJD Models is defined as follows:

The models with the below instantaneous transition rate matrix for the Markov Chain are considered:

$$\lambda_1 = \lambda_{12} = -\lambda_{11} = a\lambda, \quad \lambda_3 = \lambda_{32} = -\lambda_{33} = \frac{\lambda}{a}, \quad \lambda_{21} = \frac{ap\lambda}{(1-2p)}, \lambda_2 = \frac{(a^2+1)p\lambda}{a(1-2p)}, \lambda_{23} = \frac{p\lambda}{a(1-2p)}, \lambda_{13} = \lambda_{31} = 0. \tag{5.3.3}$$

We consider, $p < \frac{1}{2}$. The instantaneous transition rate matrix is as follows,

$$\Lambda = \begin{bmatrix} -a\lambda & a\lambda & 0 \\ \frac{ap\lambda}{(1-2p)} & -\frac{(a^2+1)p\lambda}{a(1-2p)} & \frac{p\lambda}{a(1-2p)} \\ 0 & \frac{\lambda}{a} & -\frac{\lambda}{a} \end{bmatrix}. \tag{5.3.4}$$

Additional features of the models we consider are as given below:

$$p(\mu(1) + \mu(3)) + (1 - 2p)(\mu((2)) = \overline{\overline{\mu}} \qquad (5.3.5)$$

$$p(\sigma(1) + \sigma(3)) + (1 - 2p)(\sigma((2)) = \overline{\overline{\sigma}} \qquad (5.3.6)$$

$$\overline{\overline{\sigma}} \begin{bmatrix} 1 - \epsilon \\ 1 + \epsilon \end{bmatrix} = \begin{bmatrix} \sigma_1 \\ \sigma_3 \end{bmatrix}, \text{ where, } \epsilon \in [0, 1] \qquad (5.3.7)$$

$$\overline{\overline{\mu}} = \mu(2) \qquad (5.3.8)$$

$$\overline{\overline{\sigma}} = \sigma(2) \qquad (5.3.9)$$

$$\mu(1) = \mu(3) \qquad (5.3.10)$$

The features of the smaller class of models $\mathcal{C}$ we consider result in the below theoretical implications. This way we justify our choice of a particular subset of the models from the general class of models.

The sojourn or waiting time distribution of state i, where i=1, 2, 3 is $exp(\lambda_i)$. $'a'$ is the square root of the empirical ratio of mean holding times of the high volatility regime to the low volatility regime. As the volatility process as defined in equation (4.3.2) is a continuous process, there is no possibility of the volatility of an asset to go from regime 1 to regime 3 or vice versa directly without passing through regime 2 in a model without a jump component. Therefore,

$$\lambda_{13} = \lambda_{31} = 0. \qquad (5.3.11)$$

From (5.3.3) we have,

$$\frac{\lambda_{21}}{\lambda_1} = \frac{\lambda_{23}}{\lambda_3} \text{ or, } \frac{\lambda_{21}}{\lambda_{23}} = \frac{\lambda_1}{\lambda_3} = a^2 \text{ (say)}. \qquad (5.3.12)$$

The sojourn or waiting time distribution of state i, where $i = 1, 2, 3$ is $exp(\lambda_i)$. Hence the mean holding time at state i is $1/\lambda_i$. The time spent by the chain at state i on an average is called occupation measure of i, and is given by

$$O_i = \lim_{t \to \infty} \frac{1}{t} \int_0^t 1_{\{i\}}(X_{t'}) dt'.$$

For an ergodic chain these do not depend on the initial state. Assume $X_{T_1-} = 2$, where $\{T_n\}_n$ is the increasing sequence of successive transition times. Then (5.3.11) implies that $X_{T_2} = 2$. Therefore using the regeneration,

$$O_2 = \frac{E[T_1 \mid X_{T_1-} = 2]}{E[T_2 \mid X_{T_1-} = 2]} = \frac{E[T_1 \mid X_{T_1-} = 2]}{E[T_1 + (T_2 - T_1) \mid X_{T_1-} = 2]} = \frac{E[T_1 \mid X_{T_1-} = 2]}{E[T_1 \mid X_{T_1-} = 2] + E[T_2 - T_1 \mid X_{T_1-} = 2]}$$

and for $i \neq 2$,

$$O_i = \frac{E[(T_2 - T_1)1_{\{i\}}(X_{T_1}) \mid X_{T_1-} = 2]}{E[T_2 \mid X_{T_1-} = 2]} = \frac{E[(T_2 - T_1)1_{\{i\}}(X_{T_1}) \mid X_{T_1-} = 2]}{E[T_1 \mid X_{T_1-} = 2] + E[T_2 - T_1 \mid X_{T_1-} = 2]}.$$

Moreover, $a_i := E[(T_2 - T_1)1_{\{i\}}(X_{T_1}) \mid X_{T_1-} = 2] = \frac{1}{\lambda_i} \frac{\lambda_{2i}}{\lambda_2}$ for $i \in \{1, 3\}$; and $a_2 := E[T_1 \mid X_{T_1-} = 2] = 1/\lambda_2$.

Clearly, $E[(T_2 - T_1) \mid X_{T_1-} = 2] = a_1 + a_3$. Thus we get $O_i = \frac{a_i}{\sum_{i'=1}^{3} a_{i'}}$ for each $i = 1, 2, 3$.

$$\frac{a_1}{\sum_{i=1}^{3} a_i} = p = \frac{a_3}{\sum_{i=1}^{3} a_i} \tag{5.3.13}$$

(5.3.5), (5.3.6) and (5.3.13) imply that,

1. *The long run average of drift coefficient of the continuous part matches with the time average of empirical drift $\hat{\mu}$ of the data.*

2. *The long run average of volatility process for the model matches with the time average of empirical volatility $\hat{\sigma}$ of the data.*

3. *The long run proportion of time that the volatility process stays below $\hat{F}_{\hat{\sigma}}^{\leftarrow}(p)$ is p,*

4. *The long run proportion of time that the volatility process stays above $\hat{F}_{\hat{\sigma}}^{\leftarrow}(1 - p)$ is p.*

5. *The ratio of the mean holding times in high and low volatility states in the model is equal to the corresponding empirical ratio*

Provided the volatility process is not constant.

Using the expression of strong solution, the discrete version of models corresponding to each member of $\mathcal{C}$ is given by equations (4.3.8) and (4.3.7), where,

$$\eta_i = \begin{cases} 0, & \text{with probability } \frac{1}{a^2+1} \\ 1, & \text{with probability } \frac{a^2}{a^2+1}. \end{cases}$$

We show that the discretization of a 3 state Markov chain provided above in equation (4.3.8) is indeed a discretization of a continuous three regime Markov process by the following theorem.

Theorem 5.3.1. *Consider (4.3.8) with $\eta_i \sim Bernoulli(\frac{a^2}{a^2+1})$ and $\lambda_1, \lambda_2, \lambda_3$ are $a\lambda$, $\frac{(a^2+1)p\lambda}{a(1-2p)}$ and $\frac{\lambda}{a}$ respectively, where $a > 0, 0 < p < 1/2$ and $\lambda > 0$. This is the discretization of a continuous time Markov chain on $\{1, 2, 3\}$, by time step Δ, given by the transition rate matrix,*

$$\Lambda = \begin{bmatrix} -a\lambda & a\lambda & 0 \\ \frac{ap\lambda}{(1-2p)} & -\frac{(a^2+1)p\lambda}{a(1-2p)} & \frac{p\lambda}{a(1-2p)} \\ 0 & \frac{\lambda}{a} & -\frac{\lambda}{a} \end{bmatrix}. \tag{5.3.14}$$

Proof. We recall (4.3.8) below

$$X_{i+1} = X_i + ((2 - X_i) + (-\delta_{2,X_i})^{\eta_i})P_i.$$

We can observe that, the right hand side of the above equation depends only on X_i, P_i, and η_i. By definition P_i depends only on X_i and also η_i is independent of the Markov chain X. Therefore the equation (4.3.8) generates a Markov Process. Next, we aim to show that (4.3.8) generates a discrete time Markov Process with parameters which converge to those of the continuous Markov chain of the given transition matrix.

The transition probability function of a Markov chain with the transition rate matrix Λ, is given by $P(\Delta)$ where,

$$P(\Delta) = \exp\left(\Delta\Lambda\right). \tag{5.3.15}$$

By approximating the exponential in the equation (5.3.15) and using Taylor's expansion we obtain, $P(\Delta) = I + \Lambda\Delta + o(\Delta)$, where, I is the Identity Matrix of the same dimensions of Λ. The approximated transition probabilities thus obtained is,

$$P(\Delta) = \begin{bmatrix} 1 - a\lambda\Delta & a\lambda\Delta & 0 \\ \frac{ap\lambda}{(1-2p)}\Delta & 1 - \frac{(a^2+1)p\lambda}{a(1-2p)}\Delta & \frac{p\lambda}{a(1-2p)}\Delta \\ 0 & \frac{\lambda}{a}\Delta & 1 - \frac{\lambda}{a}\Delta \end{bmatrix} + o(\Delta).$$

The first term on the right hand side, denoted by $\tilde{P}(\Delta)$, is a probability matrix since, $\Delta < \min\{1/\lambda_i | i = 1, 2, 3\}$. This implies, $\lambda_i\Delta < 1$, therefore, all the terms of $\tilde{P}(\Delta) > 0$. Finally, the equality of the transition probabilities of the discretization and the continuous version is shown. Recall that η_i and P_i are independent. From the equation (4.3.8), we can see that, there is no way that a transition can occur from regime 1 to 3 and vice versa, this is consistent with $\tilde{P}_{13}(\Delta) = \tilde{P}_{31}(\Delta) = 0$.

From (4.3.8) $P(X_{i+1} = 1 | X_i = 2) = P(P_i = 1, \eta_i = 1 | X_i = 2) = \frac{(a^2+1)p\lambda}{a(1-2p)}\Delta\frac{a^2}{a^2+1} = \frac{ap\lambda}{(1-2p)}\Delta$ which is equal to $\tilde{P}_{21}(\Delta)$. Also, from (4.3.8) $P(X_{i+1} = 3 | X_i = 2) = P(P_i = 1, \eta_i = 0 | X_i = 2) = \frac{p\lambda}{a(1-2p)}\Delta$, which is equal to $\tilde{P}_{23}(\Delta)$. Next, from (4.3.8) $P(X_{i+1} = 2 | X_i = 1) = P(P_i = 1 | X_i = 1) = a\lambda\Delta$, which is equal to $\tilde{P}_{12}(\Delta)$. Finally, from (4.3.8) $P(X_{i+1} = 2 | X_i = 3) = P(P_i = 1 | X_i = 3) = \frac{\lambda}{a}\Delta$, which is equal to $\tilde{P}_{32}(\Delta)$. Thus $\tilde{P}(\Delta)$ is indeed the transition probability matrix of $\{X_i\}_i$ in (4.3.8).

Finally, as $\Delta^{-1}(\tilde{P}(\Delta) - I)$ and $\Delta^{-1}(P(\Delta) - I)$ converge to the same limit, the result follows. □

5.3.1 Simulation Results

For simulation purposes, the parameter λ_1 is varied by taking $\frac{1}{\lambda_1 dt} = 1, 2, 3.. . , 16$ and the parameter ϵ is chosen as e_i from $e_1, e_2, ...e_{10}$ for each iteration 'i' where e_i are equispaced points from the interval $[0, 1)$.

For each index in Table 5.1 and 5.2, we set the null hypothesis,

H_0 : the law of time series is Markov modulated MJD 4.3.1 with parameters of continuous part in subclass $\mathcal{C}$. For each index, we compute the value of α_r as in the section 4.2 for $r = 1, 2, 3, 4$ by simulating 4.3.7.

Note: From hereon subclass of models of TRMJD means the subclass $\mathcal{C}$ and subclass of models of uni-regime MJD means the subclass as defined in definition 5.2.1.

For each index, α_r where, r=1, 2, 3, 4 are computed as specified in subsection 4.2.1. The results are presented in Table 5.3.

Table 5.3: The α-values for all the indices under Ternary Markov regime/TRMJD model hypotheses

Index	For $\mathscr{C}$ using $d(\hat{\sigma};p)$				For $\mathscr{C}$ using $d(-\hat{\sigma};p)$			
	α_1	α_2	α_3	α_4	α_1	α_2	α_3	α_4
I01	0.50	0.35	0.04	0.03	0.50	0.39	0.39	0.39
I02	0.47	0.46	0.09	0.08	0.49	0.37	0.37	0.37
I03	0.50	0.31	0.02	0.01	0.48	0.48	0.48	0.48
I04	0.49	0.34	0.06	0.04	0.50	0.41	0.41	0.41
I05	0.49	0.42	0.12	0.09	0.49	0.14	0.13	0.13
I06	0.50	0.40	0.19	0.15	0.49	0.28	0.28	0.28
I07	0.49	0.43	0.24	0.16	0.50	0.16	0.16	0.16
I08	0.48	0.45	0.25	0.18	0.50	0.22	0.22	0.22
I09	0.47	0.46	0.28	0.25	0.49	0.33	0.29	0.29
I10	0.49	0.42	0.31	0.26	0.49	0.40	0.28	0.28
I11	0.47	0.40	0.06	0.03	0.48	0.28	0.15	0.12
I12	0.50	0.25	0.06	0.06	0.47	0.18	0.18	0.18
I13	0.46	0.42	0.42	0.34	0.46	0.06	0.03	0.03
I14	0.48	0.46	0.24	0.16	0.47	0.15	0.15	0.15
I15	0.49	0.43	0.22	0.15	0.50	0.34	0.18	0.14
I16	0.49	0.44	0.10	0.08	0.49	0.38	0.38	0.38
I17	0.50	0.43	0.12	0.05	0.49	0.14	0.14	0.14

In Table 5.3.1 we summarize the fitting of TRMJD models. The best model class and the best parameter values are recorded in the last 4 columns. This is done based on proximity measure α_4 values obtained for members of the class $\mathcal{C}$. The largest α_4 are given in the 2nd column of the table. The model which is a member of the class $\mathcal{C}$ having the highest α_4 value is considered to be the best fit model based on the squeeze-expansion duration statistics. This best fit model is used for experiments in the next section.

Table 5.4: Model fitting using α_4 values from table

Index	α_4 value	Model Fitting		
		$\hat{\sigma}$	ϵ	$\frac{1}{\lambda_1 \Delta}$
I01	0.39	6.9%	0.76	6
I02	0.37	7.0%	0.85	5
I03	0.48	6.9%	0.66	7
I04	0.41	6.7%	0.85	5
I05	0.13	9.7%	0.85	5
I06	0.28	9.5%	0.85	5
I07	0.16	10.2%	0.85	8
I08	0.22	9.1%	0.85	5
I09	0.29	11.0%	0.85	4
I10	0.28	10.0%	0.66	8
I11	0.12	10.3%	0.85	5
I12	0.18	13.6%	0.85	5
I13	0.34	15.1%	0.57	8
I14	0.16	8.6%	0.85	5
I15	0.15	11.1%	0.76	8
I16	0.38	9.5%	0.76	7
I17	0.14	7.8%	0.85	5

5.4 Comparison of Empirical CDF of Return Distribution

Let F_1 be the eCDF of the simple return obtained from the simulation of a theoretical model and F_2 be the eCDF of the simple return from the time series data on the domain $(-\infty, \infty)$. We measure the performance of the theoretical fitted model using the L^2 error, $||F_1 - F_2||_2$, as given below.

Definition 5.4.1. *Let F_1 be eCDF of a population and F_2 be the eCDF of a fitted model. The L^2 error of the fitted model is defined as:*
$$||F_1 - F_2||_2 = \sqrt{\int_{-\infty}^{\infty} |F_1(x) - F_2(x)|^2 dx}. \quad \textit{In discrete form, } ||F_1 - F_2||_2 = \sqrt{\left(\sum_i |F_1(x_i) - F_2(x_i)|^2 |x_{i+1} - x_i|\right)}$$
where x_i's are equi-spaced points on $(\infty, -\infty)$.

The low L^2 error of a theoretical model indicates a better fitting of the empirical return distribution. The comparison of the L^2 errors of the two models (best fit uni-regime MJD and TRMJD model as specified in chapter 5 are illustrated in the figure 5.3 below.

Note: The L^2 errors are calculated over a single realization of the theoretical models.
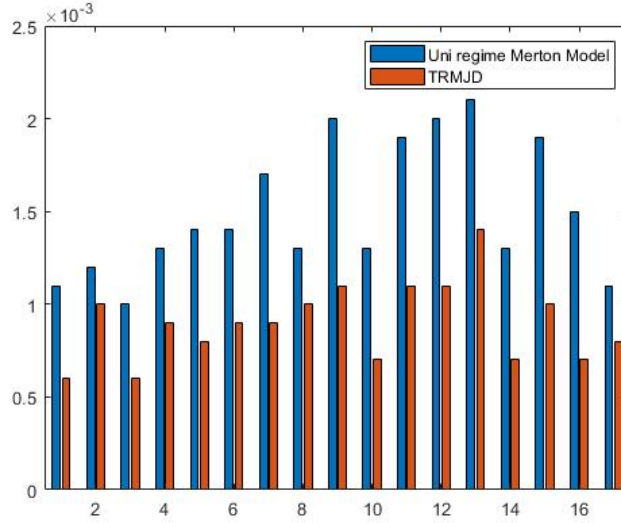
Figure 5.3: Comparison of L2 errors

We can observe that the L^2 error of the Markov switching TRMJD is lower than that of the uni-regime MJD Model. This indicates at a better performance of the Markov switching TRMJD than the uni-regime MJD model.

Note: Best fit uni regime MJD model is simulated using 4.3.5 and best fit TRMJD model is simulated using 4.3.7.

Further we also attempt to show that the difference between eCDF of the return from the simulation of the uni-regime MJD model and Markov switching TRMJD model is statistically significant using a 2 Sample Kolmogorov-Smirnov (K-S) test.

The 2 sample K-S test is defined as below.

Definition 5.4.2. *Let $F_{1,n}$ and $F_{2,m}$ be the eCDF's of two samples where 'n' and 'm' are the sizes of the 1st and 2nd samples respectively. Assume that the null hypothesis, H_0 is that the two samples come from the same underlying distribution. The Kolmogorov-Smirnov statistic for testing this hypothesis is given by, $D_{n,m} = sup_x|F_{1,n}(x) - F_{2,m}(x)|$. For large samples, the null hypothesis is rejected at level α if, $D_{n,m} > c(\alpha)\sqrt{\frac{n+m}{n.m}}$. The value of $c(\alpha)$ is given in the table 5.5.*

α	0.20	0.15	0.10	0.05	0.025	0.01	0.005	0.001
$c(\alpha)$	1.073	1.138	1.224	1.358	1.480	1.628	1.731	1.949

Table 5.5: $c(\alpha)$ values for two sample K-S test

Index	I01	I02	I03	I04	I05	I06	I07	I08	I09	I10	I11	I12	I13	I14	I15	I16	I17
$\frac{D_{n,m}}{\sqrt{\frac{n+m}{n.m}}}$	3.58	3.01	2.10	3.47	3.92	3.80	4.22	4.15	3.55	2.35	4.50	3.67	2.07	4.35	3.29	3.24	3.62

Table 5.6: K-S Test statistics for return distributions of uni-regime MJD model and Markov switching TRMJD model

The table 5.6 contains the value of '$\frac{D_{n,m}}{\sqrt{\frac{n+m}{n.m}}}$' for return distributions of uni-regime MJD model and Markov switching TRMJD model for each index. In view of this, we conclude that the respective return distributions are significantly different. This conclusion strengthens our case for the better performance of the Markov switching TRMJD model than the uni-regime MJD model.

Note: The K-S test statistics are calculated over a single realization of the theoretical models.

We also perform the K-S test between the returns obtained from the time series data and from theoretical models(uni-regime MJD or Markov switching TRMJD). The objective of this experiment is to determine whether the test statistic obtained for returns coming from time series data and the Markov switching TRMJD model is smaller than the one obtained for returns coming from time series data and uni-regime MJD model. This would demonstrate the success of the proposed Markov switching TRMJD model in replicating the empirical return distribution over the uni-regime MJD model. Given below are the test statistics values obtained from the respective K-S tests.

Index	I01	I02	I03	I04	I05	I06	I07	I08	I09	I10	I11	I12	I13	I14	I15	I16	I17
MJD	3.08	3.59	2.72	4.05	3.07	3.68	3.89	3.50	4.82	3.05	4.28	3.71	4.02	3.62	4.12	3.81	3.23
TRMJD	1.74	2.87	1.77	2.47	2.28	2.31	2.47	2.53	2.52	1.68	2.45	2.44	2.47	2.14	2.56	1.75	2.65

Table 5.7: K-S statistics between empirical and theoretical models
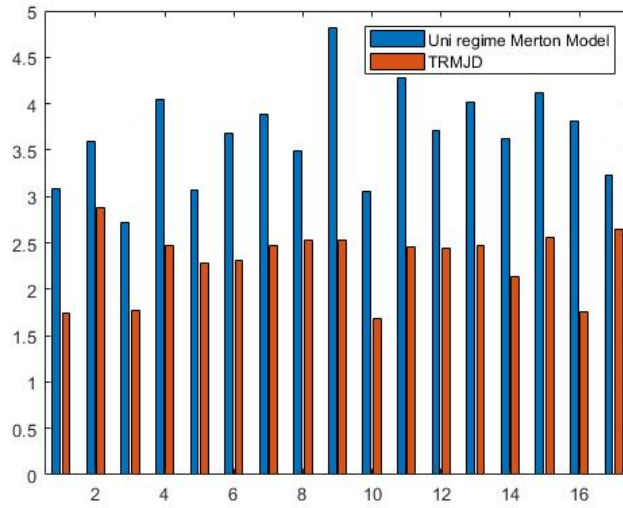
Figure 5.4: K-S test statistics of uni-regime MJD model and TRMJD model over various indices

Note: The K-S test statistics are calculated over a single realization of the theoretical models.

From the table 5.7 and figure 5.4 we can clearly observe that the test statistics of TRMJD is lesser than that of the test statistics of the uni-regime MJD model for all indices. This demonstrates the better performance of the proposed Markov switching TRMJD over the uni-regime MJD model in replicating the eCDF of the return and subsequently the return distribution obtained from the data of various indices.

Chapter 6

Conclusion

The proposed technique for jump detection proves to be a considerable success due to the high accuracy obtained across a wide range of parameter values. The regime switching model obtained using the proposed discriminating statistics demonstrates its superior performance to that of the standard uni-regime model by providing a better replication of the empirical Cumulative Distribution Function (eCDF) of the return time series data. These observations validate the efficiency of proposed regime switching model for financial asset price data. This corroborates our extension of the approach used for binary regime switching model in [33] to a ternary regime switching model.

This thesis considers a narrow sub-class of models due to the high dimensionality of the general class of models and subsequently ease of computation. On the other hand, by usage of techniques like parallel programming or running code on a cluster computer the issues of increasing dimensionality and computational complexity can be addressed. Consideration of a broader sub-class class of models is expected to result in best fit models with better discriminating statistics and performance than when a narrow sub-class of models are considered.

The technique of non parametric calibration of jumps unlike the assumption of the jumps following a log-normal distribution, as done in this work, might lead to better performance indicators such as the L_2 norm and the K-S test statistics. Although, the non parametric calibration of jumps is contingent on factors such as the granularity of the time series data and the number of jumps detected by the technique used.

To achieve enhanced performance of best fit models with respect to performance indicators such as, L_2 norm and K-S test statistics than displayed in this work by doing away with the discriminating statistics based on squeeze and expansion approach. Instead, other approaches that aim at minimizing the performance indicators, which leads to better performing models, such as, gradient descent method could be adopted.

The time spent on this thesis and insights we have gained over time has led to the ideas of new approaches to propose models that might achieve enhanced performance.

Appendices

Appendix A

Matlab Code

A.1   Historical Volatility in MMGBM

```matlab
clc
clear all
TPM=[0 0.8 0.2;0.5 0 0.5;0.3 0.7 0];%transition probability matrix
CPM=transpose(cumsum(transpose(TPM)));%cumulative probability matrix
L=[10 50 20];%input('\nEnter  n value of Lambda :')%instantaneous transition rate
    matrix
Ft=3;%no of years to be simulated
dt=1/253;%granularity
l=input('\n No of simulations of Historical Volatility :\n');
k=20;%window to  compute historical volatility
S_0=100;%initial asset price
X(1)=1;%initial state of the Markov Chain
a=0;
m=floor(Ft/dt);%no of time points
j=0;

%Antithetic simulation of Markov modulated GBM
sigma=[0.05 0.10 0.20];%volatility matrix containing volatility for three states of
     the Markov Chain
Mu=[0.02 0.08 0.04];%drift matrix containing drift for three states of the Markov
    Chain

    for i=1:l
```

```matlab
22            S_m(i,1)=100;%initial value of the asset for each simulation
23       end
24  for i=1:l
25            M=markovfun(L,TPM,dt,Ft);%generating Markov chain
26            %initialization
27            R(i,1)=0;
28            C_m_t(i,1)=0;
29            D_m_t(i,1)=0;

31            for j=1:m

33                    C_m(i,j)=(Mu(M(j))-0.5*(sigma(M(j))^2))*dt;
34                    D_m(i,j)=sigma(M(j))*sqrt(dt)*normrnd(0,1);
35                    C_m_t(i,j+1)=C_m_t(i,j)+C_m(i,j);
36                    D_m_t(i,j+1)=D_m_t(i,j)+D_m(i,j);
37                    ST_m(i,j)=S_0*exp(C_m_t(i,j+1)+D_m_t(i,j+1));%simulated asset price
38                    P(i,j)=sigma(M(j));%volatility of state of Markov chain at time
                         point 'j'

40                    if j>1
41                    R(i,j)=((ST_m(i,j)-ST_m(i,j-1))/ST_m(i,j-1));%simple return
42                    end

44                    if j>=k
45                        W=R(i,j-k+1:j);%return for a given window of size k
46                        E= sum(R(i,j-k+1:j));
47                        V(i,j)=((sum(W.^2)/k)-((E/k)^2))/dt;%historical variance for
                             window size k
48                        v(i,j)=(V(i,j))^0.5;%historical volatility for window size k
49                    else
50                        V(i,j)=0;
51                        v(i,j)=0;
52                    end
53            end
54  end
55  T=1:m;%time matrix
56  for i=1:l
57      plot(T,v(i,:))%plotting of historical volatility

59      hold on
60      plot(T,P(i,:))%plotting of volatility of state of Markov chain at time 'i'
61  end
```

A.2   Calculation of Jump accuracy for a Uni-Regime MJD

```
1    clear
2   beta=[0.01 0.1 0.2 0.3 0.4 0.5 0.6 0.7 0.8]; %The volatility (beta) matrix
3   N_b=size(beta,2);
4   jmax=20; %Number of simulations for each beta
5   pi=2*asin(1.0);
6   N=18000;%Length of the time series
7   N2=N/2;
8   dt=5./(250*360);   %Granularity
9   d_t=sqrt(dt);
10  T=N*dt;
11  mu=0.1;
12  del=0.0055;
13  %del=10*del;
14  lamb=100;
15  ga=-((del^2)/2); %to keep the mean jump size zero
16  plamb=1-(exp(-lamb*dt)); %probability of observing at least one jump in dt time-
        length
17
18  alpha=(0.5)*10^40; % alpha=(0.5)*10^40 gives \hat{p}=1.0122%
19  ph=min(1,alpha*(dt^(log(1/dt)))); %\hat{p} value
20  g=sqrt(dt)*norminv((1+((1-ph)^(1/N)))/2); %g is \gamma
21
22  acc1=zeros(N_b,jmax);
23  acc2=zeros(3,N_b,jmax);
24  acc_1=zeros(1,N_b);
25  acc_2=zeros(3,N_b);
26  for k=1:N_b % For each k a separate beta is chosen.
27  sig=beta(k);
28  for j=1:jmax
29 %For each j, a simulation and accuracy of jump classification is computed. Then
        average accuracy is computed for each beta.
30  W=zeros(1,N+1);
31  W(1)=0;
32  for i=1:N2      %Brownian motion
33      u1=rand(); %by Box Muller Method
34      u2=rand();
```

44

```matlab
35      W(2*i)=W(2*i-1)+sqrt(dt*(-2)*log(1-u1))*cos(2*pi*u2);%Simulating Brownian
           motion
36      W(2*i+1)=W(2*i)+sqrt(dt*(-2)*log(1-u1))*sin(2*pi*u2);
37  end
38
39  S=zeros(1,N+1); %Asset time series initialization
40  S(1)=1;         %Initial Asset price
41  Xi=zeros(1,N);
42  for i=1:N       %Simulation using above W and following Xi.
43      u1=rand();
44      if u1 <= plamb    % then jump happens
45          u1=rand();    % Generating Jump Size (Merton Model)
46          u2=rand();    % Jump size is LogNormal -1
47          Xi(i)=exp(ga+del*sqrt((-2)*log(1-u1))*cos(2*pi*u2))-1;
48      else              % else jump does not occur
49          Xi(i)=0;      % so Xi(i) =0
50      end
51      S(i+1)=S(i)*(1+mu*dt+sig*(W(i+1)-W(i))+Xi(i));% Simulating the asset pricing
           model
52  end                   %Simulation is complete.
53
54  S_l=log(S);
55  ret_l=diff(S_l);  %This is the log return series
56  ret_l=(ret_l).^2; %Square of log return series
57  ret=diff(S)./S(1:N);       %This is the simple return series
58  n=size(ret,2);
59
60  r_s=std(ret);      %This is denoted as SD
61  m_r=mean(ret);    %This is \bar{r}
62
63  %Next we solve an implicit equation to compute the maximal estimator of \beta, and
       thereby the maximal threshold
64  y=10;                     %Number of iteration
65  b=zeros(1,y);
66  b(1)=r_s/sqrt(2*dt);   %initial value of beta for N-R iteration
67  c_h(1)=g*b(1);         %initial value of threshold c_h
68
69  for i=1:y-1               %Solving F1=0 by N-R iteration.
70      F1=((b(i))^2)-((1/T)*((sum((ret-m_r).^2))-(sum(ret(abs(ret-m_r)>(b(i)*g)).^2)))
           ); %The functional F1
71      b(i+1)=b(i)-(F1/(2*b(i)));          %N-R iteration scheme
72  end
```

45

```matlab
73
74  c=g*b(y);                              %Maximal Threshold
75  ret_h=ret(abs(ret-m_r)>(c));           %The series of jump sizes
76  L=sum(abs(ret-m_r)>(c))/(n*dt);        %\Lambda, the intensity
77  v=sum((ret_h-m_r).^2)/((L*n*dt)-1);%Variance of jump sizes
78
79  ret_h1=(Xi~=0); %identifying instances where jump has occurred in simulation data
80  ret_h2=((abs(ret-m_r))>c); %estimating instances where jump has occurred using
        maximal threshold (output=boolean array)
81
82  truepos1=sum(ret_h2(ret_h2==ret_h1));
83  trueneg1=sum(abs(ret_h2(ret_h2==ret_h1)-1));
84  acc1(k,j)=(truepos1+trueneg1)/(N);
85
86  for iter =1:3
87      power=1-10^(-iter); % power = 0.9, 0.99, 0.999
88      c_m=((dt)^power);
89  ret_h4=(ret_l > c_m);%identifying instances where jump has occurred(using Mancini's
        threshold)
90  truepos2=sum(ret_h4(ret_h4==ret_h1));
91  trueneg2=sum(abs(ret_h4(ret_h4==ret_h1)-1));
92  acc2(iter,k,j)=(truepos2+trueneg2)/(N);
93  end
94  end
95  %[sum(ret_h1),sum(ret_h2),truepos1] % for checking
96  acc_1(k)=mean(acc1(k,:));%Mean accuracy of maximal threshold
97  for iter =1:3
98  acc_2(iter,k)=mean(acc2(iter,k,:));%Mean accuracy of standard threshold
99  end
100 end
101 %plotting of jump accuracy
102 plot(beta,acc_1,'Color', [1 0 0.9], 'LineWidth',2)
103 hold on
104 h=plot(beta,acc_2,'LineWidth',2);
105 set(h,{'Color'}, {[1 0 0]; [0 1 0]; [0 0 1]});
```

A.3   Calculation of Jump accuracy for a Ternary Regime Markov Switching MJD

```matlab
1    clear
2    beta=[0.01  0.1  0.2  0.3  0.4  0.5  0.6  0.7  0.8]; %The volatility (beta) matrix
3    N_b=size(beta,2);
4    jmax=1000; %Number of simulations for each beta
5    pi=2*asin(1.0);
6    N=11000;%Length of the time series
7    N2=N/2;
8    dt=5./(250*360);   %Granularity
9    d_t=sqrt(dt);
10   T=N*dt;
11
12   J=[ 0.08   150    2.0e−05     0.07  ];%parameter matrix
13
14   eps=0.8 ;%parameter used in the volatility matrix
15   l_m=1.0e+03 *[ 3.0000    1    2.5];%Instantaneous transition rates
16   a=sqrt(3/2.5);%asymmetry parameter/ratio between the transition rate of Markov
         regime 1 and 3
17   mu=J(1);%beta
18   lamb=J(2);%lambda
19   V=J(3);%Variance of jump sizes
20   mu_bar=J(4);%mean of empirical drift
21
22   % eps=eps;
23   % l_m=l_m;
24
25   del=sqrt(log(V+1));
26   ga=−((del^2)/2); %to keep the mean jump size zero
27   plamb=1−(exp(−lamb*dt)); %probability of observing at least one jump in dt time−
         length
28
29   alpha=(0.5)*10^40; % alpha=(0.5)*10^40 gives \hat{p}=1.0122%
30   ph=min(1,alpha*(dt^(log(1/dt)))); %\hat{p} value
31   g=sqrt(dt)*norminv((1+((1−ph)^(1/N)))/2); %g is \gamma
32
33   acc1=zeros(N_b,jmax);
34   acc2=zeros(3,N_b,jmax);
35   acc_1=zeros(1,N_b);
36   acc_2=zeros(3,N_b);
```

```matlab
37
38  mu_m=mu_bar*ones(1,3);%Generating the drift matrix (drift pertaining to each regime
         of the Markov Chain)
39
40  x=[];%intialization step for generating a Markov chain
41  x=mrk3(N,dt,a,l_m);%generation of Markov chain
42  W=zeros(1,N+1);
43  W(1)=0;
44
45  for k=1:N_b
46      sg_bar=beta(k);% For each k a separate beta is chosen.
47      sig_m=sg_bar*[1-eps,1,1+eps];%Generating the volatility matrix (volatility
             pertaining to each regime of the Markov Chain)
48  for j=1:jmax
49  %For each j, a simulation and accuracy of jump classification is computed. Then
        average accuracy is computed for each beta.
50  W=zeros(1,N+1);
51  W(1)=0;
52  for i=1:N2       %Brownian motion
53      u1=rand(); %by Box Muller Method
54      u2=rand();
55      W(2*i)=W(2*i-1)+sqrt(dt*(-2)*log(1-u1))*cos(2*pi*u2);%Simulating Brownian
             motion
56      W(2*i+1)=W(2*i)+sqrt(dt*(-2)*log(1-u1))*sin(2*pi*u2);
57  end
58
59  S=zeros(1,N+1); %Asset time series initialization
60  S(1)=1;          %Initial Asset price
61  Xi=zeros(1,N);
62  for i=1:N        %Simulation using above W and following Xi.
63      u1=rand();
64      if u1 <= plamb    % then jump happens
65          u1=rand();     % Generating Jump Size (Merton Model)
66          u2=rand();     % Jump size is LogNormal -1
67          Xi(i)=exp(ga+del*sqrt((-2)*log(1-u1))*cos(2*pi*u2))-1;
68      else              % else jump does not occur
69          Xi(i)=0;       % so Xi(i) =0
70      end
71      S(i+1)=S(i)*(1+mu_m(x(i))*dt+sig_m(x(i))*(W(i+1)-W(i))+Xi(i));%simulation of
             the Ternary Regime Markov Switching Merton Jump diffusion model(TRMJD)
72  end                    %Simulation is complete.
73
```

```matlab
74  S_l=log(S);
75  ret_l=diff(S_l);  %This is the log return series
76  ret_l=(ret_l).^2; %Square of log return series
77  ret=diff(S)./S(1:N);        %This is the simple return series
78  n=size(ret,2);
79
80  r_s=std(ret);       %This is denoted as SD
81  m_r=mean(ret);     %This is \bar{r}
82
83  %Next we solve an implicit equation to compute the maximal estimator of \beta, and
       thereby the maximal threshold
84  y=10;                  %Number of iteration
85  b=zeros(1,y);
86  b(1)=r_s/sqrt(2*dt);  %initial value of beta for N-R iteration
87  c_h(1)=g*b(1);         %initial value of threshold c_h
88
89  for i=1:y-1             %Solving F1=0 by N-R iteration.
90      F1=((b(i))^2)-((1/T)*((sum((ret-m_r).^2))-(sum(ret(abs(ret-m_r)>(b(i)*g)).^2)))
          ); %The functional F1
91      b(i+1)=b(i)-(F1/(2*b(i)));           %N-R iteration scheme
92  end
93
94  c=g*b(y);                        %Maximal Threshold
95  ret_h=ret(abs(ret-m_r)>(c));        %The series of jump sizes
96  L=sum(abs(ret-m_r)>(c))/(n*dt);    %\Lambda, the intensity
97  v=sum((ret_h-m_r).^2)/((L*n*dt)-1);%Variance of jump sizes
98
99  ret_h1=(Xi~=0); %identifying instances where jump has occurred in simulation data
100 ret_h2=((abs(ret-m_r))>c); %estimating instances where jump has occurred using
      maximal threshold (output=boolean array)
101
102 truepos1=sum(ret_h2(ret_h2==ret_h1));
103 trueneg1=sum(abs(ret_h2(ret_h2==ret_h1)-1));
104 acc1(k,j)=(truepos1+trueneg1)/(N);
105
106 for iter =1:3
107     power=1-10^(-iter); % power = 0.9, 0.99, 0.999
108     c_m=((dt)^power);
109 ret_h4=(ret_l > c_m);%identifying instances where jump has occurred(using Mancini's
       threshold)
110 truepos2=sum(ret_h4(ret_h4==ret_h1));
111 trueneg2=sum(abs(ret_h4(ret_h4==ret_h1)-1));
```

```
112  acc2(iter,k,j)=(truepos2+trueneg2)/(N);
113  end
114  end
115  %[sum(ret_h1),sum(ret_h2),truepos1] % for checking
116  acc_1(k)=mean(acc1(k,:));%Mean accuracy of maximal threshold
117  for iter =1:3
118  acc_2(iter,k)=mean(acc2(iter,k,:));%Mean accuracy of standard threshold
119  end
120  end
121  %plotting of jump accuracy
122  plot(beta,acc_1,'Color', [1 0 0.9], 'LineWidth',2)
123  hold on
124  h=plot(beta,acc_2,'LineWidth',2);
125  set(h,{'Color'}, {[1 0 0]; [0 1 0]; [0 0 1]});
```

A.4 Calculation of Discriminating Statistics

```
1   %Jump detection and obtaining the best fit ternary regime Markov switching Jump
        diffusion model
2
3   sheet='name of the index';%for example sheet='NIFTY200'
4   s = xlsread('niftyidxcl.xlsx',sheet);
5   s=transpose(s);%transposing the asset price time series
6   N=size(s,2);%length of the time series
7   p=15/100;%setting up 'pth' percentile for calculation of durations
8   s=flip(s);%ordering of time series from old to new
9   ret=sr(s);%calculating simple return of asset
10  r_p=prctile(ret,p*100);%calculating (100*p)th percentile of return data
11  r_s=sd(ret);%calculating standard deviation of return
12  m_r=mean(ret);%calculating mean  of return
13  n=size(ret,2);%size of return time series
14  dt=5./(250*360);%granularity
15  T=N*dt;%Total time frame of time series
16  alpha=(0.5)*10^40; % alpha=(0.5)*10^40 gives \hat{p}=1.0122%
17  ph=min(1,alpha*(dt^(log(1/dt)))); %\hat{p} value
18  d_t=sqrt(dt);%square root of granularity
19  g=sqrt(dt)*norminv((1+((1-ph)^(1/N)))/2);%g is \gamma
20  b(1)=r_s/sqrt(2*dt);%Next we solve an implicit equation to compute the maximal
        estimator of \beta, and thereby the maximal threshold
```

```matlab
21  F1(1)=((b(1))^2)−((1/T)*((sum((ret−m_r).^2))−(sum(ret(abs(ret−m_r)>(b(1)*g)).^2))))
        ;%Initial value of the functional F1
22  y=10; %Number of iterations
23  v(1)=0;
24  L(1)=0;
25  c_h(1)=g*b(1);
26
27  for i=2:y %no of iterations
28      b(i)=b(i−1)−(F1(i−1)/(2*b(i−1)));%N−R iteration scheme
29      F1(i)=((b(i))^2)−((1/T)*((sum((ret−m_r).^2))−(sum(ret(abs(ret−m_r)>(b(i)*g))
            .^2))));%The functional F1
30      c_h(i)=g*b(i); %iteration of the maximal threshold
31      ret_h=ret(abs(ret−m_r)>(c_h(i)));%Iteration of the series of jump sizes
32      L(i)=sum(abs(ret−m_r)>(c_h(i)))/(n*dt);%\Lambda, the intensity
33      v(i)=sum((ret_h−m_r).^2)/((L(i)*n*dt)−1);%Variance of jump sizes
34
35  end
36  c=g*b(y);%Maximal Threshold
37
38  %replacing the data in return time series where a jump has occurred  with the mean
        of the return
39  for i=1:n
40      if ((abs(ret(i)−m_r))<=c)
41          ret_f(i)=ret(i);
42      elseif((abs(ret(i)−m_r))>c)
43          ret_f(i)=m_r;
44      end
45  end
46  N=n;
47  w=20;%setting of window size for calculating moving average and sample standard
        deviation
48  n_f=size(ret_f,2);%size of return time series
49  for j=1:(n_f−w+1)
50      m(j)=((sum(ret_f(j:j+w−1)))/w);% moving average
51      sg(j)=sqrt((sum(ret_f(j:j+w−1).^2))/(w−1)−((w*(m(j).^2))/(w−1)));%sample
            standard deviation
52  end
53  m=m/dt;%empirical drift
54  mu_bar=(mean(m));%mean of empirical drift
55  sg=sg./sqrt(dt);%empirical volatility
56  sg_bar=mean(sg);%mean of empirical volatility
57
```

```matlab
58  dura_d=dura(sg,p*100); %durations of p−squeeze
59  dura_m=dura_mi(sg,p*100);%durations of p−expansions
60
61   L_d=size(dura_d,2);%Length of p−squeeze vector
62   T1_e1=((sum(dura_d))/L_d);%T1 descriptive statistic of p−squeeze
63   T2_e1= sqrt(sum((dura_d−T1_e1).^2)/(L_d−1));%T2 descriptive statistic of p−squeeze
64   T3_e1=(sum((dura_d−T1_e1).^3)/(L_d))/((T2_e1)^3);%T3 descriptive statistic of p−
         squeeze
65   T4_e1=(sum((dura_d−T1_e1).^4)/(L_d))/((T2_e1)^4);%T4 descriptive statistic of p−
         squeeze
66
67   L_m=size(dura_m,2);%Length of p−expansion vector
68   T1_e2=((sum(dura_m))/L_m);%T1 descriptive statistic of p−expansion
69   T2_e2= sqrt(sum((dura_m−T1_e2).^2)/(L_m−1));%T2 descriptive statistic of p−
         expansion
70   T3_e2=(sum((dura_m−T1_e2).^3)/(L_m))/((T2_e2)^3);%T3 descriptive statistic of p−
         expansion
71   T4_e2=(sum((dura_m−T1_e2).^4)/(L_m))/((T2_e2)^4);%T4 descriptive statistic of p−
         expansion
72
73  a=sqrt((T1_e2)/(T1_e1));%calculation of the parameter of asymmetry
74  B=100;%no of time series to be sampled from sub class of models of  the uni−regime
       MJD models
75
76  %Simulation of uni−regime MJD
77  for  j=1:B
78      S_g=s(1);%setting the first data point of the asset data time series as the
            initial point for simulation of sub class uni−regime MJD
79
80      gmb=gsm(S_g,dt,N,mu_bar,sg_bar);%simulation of sub class of uni−regime MJD
            models
81
82      ret_g=sr(gmb);%return of uni−regime MJD
83      n_g=size(ret_g,2);%size of return time series obtained from simulation of uni−
            regime MJD
84      for  k=1:(n_g−w+1)
85          m_g(k)=(((sum(ret_g(k:k+w−1)))/w));% moving average
86          sg_g(k)=(sqrt((sum(ret_g(k:k+w−1).^2))/(w−1)−((w*(m_g(k).^2))/(w−1))));%
                sample standard deviation
87      end
88
89      m_g=(m_g)/dt;%empirical drift
```

```matlab
90        sg_g=(sg_g)/sqrt(dt);%empirical volatility
91
92        dura_g1=dura(sg_g,p*100);%durations of p-squeeze
93        dura_g2=dura_mi(sg_g,p*100);%durations of p-expansions
94
95         L_g1=size(dura_g1,2);%Length of p-squeeze vector
96         L_g2=size(dura_g2,2);%Length of p-expansions
97
98        T1_g1(j)=((sum(dura_g1))/L_g1);%T1 descriptive statistic of p-squeeze
99        T2_g1(j)= sqrt(sum((dura_g1-T1_g1(j)).^2)/(L_g1-1));%T2 descriptive statistic
              of p-squeeze
100       T3_g1(j)=(sum((dura_g1-T1_g1(j)).^3)/(L_g1))/((T2_g1(j))^3);%T3 descriptive
              statistic of p-squeeze
101       T4_g1(j)=(sum((dura_g1-T1_g1(j)).^4)/(L_g1))/((T2_g1(j))^4);%T4 descriptive
              statistic of p-squeeze
102
103       T1_g2(j)=((sum(dura_g2))/L_g2);%T1 descriptive statistic of p-expansion
104       T2_g2(j)= sqrt(sum((dura_g2-T1_g2(j)).^2)/(L_g2-1));%T2 descriptive statistic
              of p-expansion
105       T3_g2(j)=(sum((dura_g2-T1_g2(j)).^3)/(L_g2))/((T2_g2(j))^3);%T3 descriptive
              statistic of p-expansion
106       T4_g2(j)=(sum((dura_g2-T1_g2(j)).^4)/(L_g2))/((T2_g2(j))^4);%T4 descriptive
              statistic of p-expansion
107 end
108 %Note:proximity measure statistics will be referred to as \alpha statistics
        henceforth
109 ag=[];
110 z_g1=T1_g1;
111 D1_g=((z_g1-T1_e1)<=0);
112 s_g1=sum(D1_g);
113 E1_g= g_b(s_g1,B);% g_B function on t statistics
114 ag=[ag,E1_g];
115 a1_g=min(ag);%calculation of \alpha_1 statistic pertaining to  p-squeeze of uni-
        regime MJD
116
117 z_g2=T2_g1;
118 D2_g=((z_g2-T2_e1)<=0);
119 s_g2=sum(D2_g);
120 E2_g= g_b(s_g2,B);% g_B function on t statistics
121 ag=[ag,E2_g];
122 a2_g=min(ag);%calculation of \alpha_2 statistic pertaining to  p-squeeze of uni-
        regime MJD
```

```matlab
123
124  z_g3=T3_g1;
125  D3_g=((z_g3-T3_e1)<=0);
126  s_g3=sum(D3_g);
127  E3_g= g_b(s_g3,B);% g_B function on t statistics
128  ag=[ag,E3_g];
129  a3_g=min(ag);%calculation of \alpha_3 statistic pertaining to p-squeeze of uni-
         regime MJD
130
131  z_g4=T4_g1;
132  D4_g=((z_g4-T4_e1)<=0);
133  s_g4=sum(D4_g);
134  E4_g= g_b(s_g4,B);% g_B function on t statistics
135  ag=[ag,E4_g];
136  a4_g=min(ag);%calculation of \alpha_4 statistic pertaining to  p-squeeze of uni-
         regime  MJD
137
138  %\alpha statistics of p-squeeze of uni-regime MJD
139  alpha(1)=a1_g;
140  alpha(2)=a2_g;
141  alpha(3)=a3_g;
142  alpha(4)=a4_g;
143
144  ah=[];
145  z_h1=T1_g2;
146  D1_h=((z_h1-T1_e2)<=0);
147  s_h1=sum(D1_h);
148  E1_h= g_b(s_h1,B);% g_B function on t statistics
149  ah=[ah,E1_h];
150  a1_h=min(ah);%calculation of \alpha_1 statistic pertaining to  p-expansion of uni-
         regime MJD
151
152  z_h2=T2_g2;
153  D2_h=((z_h2-T2_e2)<=0);
154  s_h2=sum(D2_h);
155  E2_h= g_b(s_h2,B);% g_B function on t statistics
156  ah=[ah,E2_h];
157  a2_h=min(ah);%calculation of \alpha_2 statistic pertaining to  p-expansion of uni-
         regime MJD
158
159  z_h3=T3_g2;
160  D3_h=((z_h3-T3_e2)<=0);
```

```matlab
161  s_h3=sum(D3_h);
162  E3_h= g_b(s_h3,B);% g_B function on t statistics
163  ah=[ah,E3_h];
164  a3_h=min(ah);%calculation of \alpha_3 statistic pertaining to p−expansion of uni−
         regime MJD
165
166  z_h4=T4_g2;
167  D4_h=((z_h4−T4_e2)<=0);
168  s_h4=sum(D4_h);
169  E4_h= g_b(s_h4,B);% g_B function on t statistics
170  ah=[ah,E4_h];
171  a4_h=min(ah);%calculation of \alpha_4 statistic pertaining to p−expansion of uni−
         regime MJD
172
173  %\alpha statistics pertaining to p−expansion of uni−regime MJD
174  alpha(5)=a1_h;
175  alpha(6)=a2_h;
176  alpha(7)=a3_h;
177  alpha(8)=a4_h;
178
179  mu=mu_bar*ones(1,3);%Drift vector pertaining to the sub class of TRMJD model
180  g=abs(linspace(0,0.85,10));%setting up of epsilon parameter required for volatility
         vector of sub class of TRMJD model
181
182  %let \theta be a member of the parameter set of sub class TRMJD models
183
184  for i=1:10
185      eps=g(i);%selection of epsilon from the vector (selection of a member from the
             parameter set of sub class of models)
186      sg_mg=sg_bar*[1−eps,1,1+eps];%generation of volatility vector (selection of a
             member from the parameter set of sub class of models)
187      for j=1:16
188          l_m=[];
189          %generation of instantaneous transition rate matrix for a ternary regime
                 Markov process (for a given \theta)
190          l=(((1)/(j))/(dt))/(a);
191          l_11(j)=(a*l) ;l_33(j)=(l/a);
192          l_22(j)=((((a^2)+1)*p*l)/(a*(1−2*p)));
193          l_m=[l_11(j),l_22(j),l_33(j)];
194
195
```

```matlab
196            S_m=s(1);%setting the first data point of the asset data time series as the
                   initial point for simulation of Ternary regime switching MJD (TRMJD)
197
198            for k=1:100%simulation of TRMJD(for a given \theta i.e. member of the sub
                   class) k times
199
200                sm=mgbm_1(S_m,N,dt,a,l_m,mu,sg_mg);%simulation of TRMJD(for a given \
                       theta i.e. member of the sub class)
201                ret_m=sr(sm);%return of TRMJD
202                n_m=size(ret_m,2);%size of return time series obtained from simulation
                       of TRMJD
203
204                for t=1:(n_m-w+1)
205                    m_m(t)=(((sum(ret_m(t:t+w-1)))/w));% moving average
206                    sg_m(t)=(sqrt(((sum(ret_m(t:t+w-1).^2))/(w-1))-((w*(m_m(t).^2))/(w
                           -1)))) ;%sample standard deviation
207                end
208                m_m=(m_m)/dt;%empirical drift
209                sg_m=(sg_m)/sqrt(dt);%empirical volatility
210
211                dura_m1{i,j,k}=dura(sg_m,p*100);%duration of p-squeeze
212                dura_m2{i,j,k}=dura_mi(sg_m,p*100);%duration of p-expansion
213
214                L_m1(i,j,k)=size(dura_m1{i,j,k},2);%Length of p-squeeze vector
215                L_m2(i,j,k)=size(dura_m2{i,j,k},2);%Length of p-expansion vector
216
217                T1_m1(i,j,k)=((sum(dura_m1{i,j,k}))/L_m1(i,j,k));%T1 descriptive
                       statistic of p-squeeze
218                T2_m1(i,j,k)= sqrt(sum((dura_m1{i,j,k}-T1_m1(i,j,k)).^2)/(L_m1(i,j,k)
                       -1));%T2 descriptive statistic of p-squeeze
219                T3_m1(i,j,k)=(sum((dura_m1{i,j,k}-T1_m1(i,j,k)).^3)/(L_m1(i,j,k)))/((
                       T2_m1(i,j,k))^3);%T3 descriptive statistic of p-squeeze
220                T4_m1(i,j,k)=(sum((dura_m1{i,j,k}-T1_m1(i,j,k)).^4)/(L_m1(i,j,k)))/((
                       T2_m1(i,j,k))^4);%T4 descriptive statistic of p-squeeze
221
222                T1_m2(i,j,k)=((sum(dura_m2{i,j,k}))/L_m2(i,j,k));%T1 descriptive
                       statistic of p-expansion
223                T2_m2(i,j,k)= sqrt(sum((dura_m2{i,j,k}-T1_m2(i,j,k)).^2)/(L_m2(i,j,k)
                       -1));%T2 descriptive statistic of p-expansion
224                T3_m2(i,j,k)=(sum((dura_m2{i,j,k}-T1_m2(i,j,k)).^3)/(L_m2(i,j,k)))/((
                       T2_m2(i,j,k))^3);%T3 descriptive statistic of p-expansion
```

```
225          T4_m2( i , j , k)=(sum ( ( dura_m2{ i , j , k}−T1_m2( i , j , k ) ) . ^ 4 ) / ( L_m2( i , j , k ) ) ) / ( (
                T2_m2( i , j , k ) ) ^ 4 ) ;%T4 descriptive statistic of p−expansion
226      end
227
228      z_m1=T1_m1( i , j , : ) ;
229      am1 = [ ] ;
230      D1_m1=(( z_m1−T1_e1)<=0);
231      s_m1=sum ( D1_m1 ) ;
232      E1_m1= g_b ( s_m1 ,B) ;
233      am1=[am1 , E1_m1 ] ;
234      a1_m1=min (am1 ) ;%calculation of \alpha_ (1 , \ theta ) statistic pertaining to   p
             −squeeze of TRMJD
235
236      z_m2=T2_m1( i , j , : ) ;
237      D2_m1=(( z_m2−T2_e1)<=0);
238      s_m2=sum ( D2_m1 ) ;
239      E2_m1= g_b ( s_m2 ,B) ;% g_B function on t statistics
240      am1=[am1 , E2_m1 ] ;
241      a2_m1=min (am1 ) ;%calculation of \alpha_ (2 , \ theta ) statistic pertaining to   p
             −squeeze of TRMJD
242
243      z_m3=T3_m1( i , j , : ) ;
244      D3_m1=(( z_m3−T3_e1)<=0);
245      s_m3=sum ( D3_m1 ) ;
246      E3_m1= g_b ( s_m3 ,B) ;% g_B function on t statistics
247      am1=[am1 , E3_m1 ] ;
248      a3_m1=min (am1 ) ;%calculation of \alpha_ (3 , \ theta ) statistic pertaining to   p
             −squeeze of TRMJD
249
250      z_m4=T4_m1( i , j , : ) ;
251      D4_m1=(( z_m4−T4_e1)<=0);
252      s_m4=sum ( D4_m1 ) ;
253      E4_m1= g_b ( s_m4 ,B) ;% g_B function on t statistics
254      am1=[am1 , E4_m1 ] ;
255      a4_m1=min (am1 ) ;%calculation of \alpha_ (4 , \ theta ) statistic pertaining to   p
             −squeeze of TRMJD
256
257      %alpha statistics pertaining to  p−squeeze of TRMJD( one member of the sub
             class )
258      a1_m2( i , j )=a1_m1 ;
259      a2_m2( i , j )=a2_m1 ;
260      a3_m2( i , j )=a3_m1 ;
```

```matlab
261                a4_m2(i,j)=a4_m1;
262
263                z_n1=T1_m2(i,j,:);
264                an1=[];
265                D1_n1=((z_n1-T1_e2)<=0);
266                s_n1=sum(D1_n1);
267                E1_n1= g_b(s_n1,B);% g_B function on t statistics
268                an1=[an1,E1_n1];
269                a1_n1=min(an1);%calculation of \alpha_(1,\theta) statistic pertaining to  p
                       -expansion of TRMJD
270                z_n2=T2_m2(i,j,:);
271                D2_n1=((z_n2-T2_e2)<=0);
272                s_n2=sum(D2_n1);
273                E2_n1= g_b(s_n2,B);% g_B function on t statistics
274                an1=[an1,E2_n1];
275                a2_n1=min(an1);%calculation of \alpha_(2,\theta) statistic pertaining to  p
                       -expansion of TRMJD models
276
277                z_n3=T3_m2(i,j,:);
278                D3_n1=((z_n3-T3_e2)<=0);
279                s_n3=sum(D3_n1);
280                E3_n1= g_b(s_n3,B);% g_B function on t statistics
281                an1=[an1,E3_n1];
282                a3_n1=min(an1);%calculation of \alpha_(3,\theta) statistic pertaining to  p
                       -expansion of TRMJD models
283
284                z_n4=T4_m2(i,j,:);
285                D4_n1=((z_n4-T4_e2)<=0);
286                s_n4=sum(D4_n1);
287                E4_n1= g_b(s_n4,B);% g_B function on t statistics
288                an1=[an1,E4_n1];
289                a4_n1=min(an1);%calculation of \alpha_(4,\theta) statistic pertaining to  p
                       -expansion of TRMJD models
290
291            % \alpha statistic pertaining to  p-expansion of TRMJD models
292                a1_n2(i,j)=a1_n1;
293                a2_n2(i,j)=a2_n1;
294                a3_n2(i,j)=a3_n1;
295                a4_n2(i,j)=a4_n1;
296        end
297    end
298    a1_m=max(max(a1_m2));
```

```matlab
299  a2_m=max(max(a2_m2));
300  a3_m=max(max(a3_m2));
301  a4_m=max(max(a4_m2));
302
303  %\alpha statistics pertaining to p-squeeze  of TRMJD models(considering the whole
         sub class)
304  alpha(9)=a1_m;
305  alpha(10)=a2_m;
306  alpha(11)=a3_m;
307  alpha(12)=a4_m;
308
309  a1_n=max(max(a1_n2));
310  a2_n=max(max(a2_n2));
311  a3_n=max(max(a3_n2));
312  a4_n=max(max(a4_n2));
313  %\alpha statistics pertaining to p-expansion  of TRMJD(considering the whole sub
         class)
314  alpha(13)=a1_n;
315  alpha(14)=a2_n;
316  alpha(15)=a3_n;
317  alpha(16)=a4_n;
318  alpha_ternary=alpha(9:16);
319  sheet=1;
320  xlswrite(filename,alpha_ternary,sheet,'Am:Hm');% 'm' is the index number
```

A.5 Simulation of Best Fit Model for Calculation of L_2 Error and K-S Test Statistics

```matlab
1   %simulation of the best fit model for calculation of L2 error and K–S test
        statistics
2
3
4   J1 = xlsread('modelstats.xlsx');% 'modelstats.xlsx' contains the parameters for the
        best fit model'
5   J=J1(m,1:10);% 'm' is the index 'im' corresponding to which the best fit model is
        being simulated m=1,...,17
6   J=array2table(J);
7   sheet='name of the index';%for example sheet='NIFTY200'
8   s = xlsread('niftyidxcl.xlsx',sheet);%reading the asset price data of the index
9   s=table2array(s);
10  s=transpose(s);%transposing the asset price time series
11  s=flip(s);%ordering of time series from old to new
12  ret=sr(s);%calculating simple return of asset
13  ret=sort(ret);%sorting of the return time series
14  N=size(s,2);%Length of the time series
15  pi=2*asin(1.0);
16  N=size(s,2);%Length of the time series
17  N2=ceil(N/2);
18  dt=5./(250*360);  %Granularity
19  d_t=sqrt(dt);%square root of granularity
20  T=N*dt;%Total time frame of time series
21  eps=J(6); %epsilon parameter of the best fit  TRMJD model for a given index
22  a=J(7);%asymmetry parameter of the best fit TRMJD model for a given index
23  l_m=[J(8) J(9) J(10)];%instantaneous transition rates of best fit TRMJD model
24  %feeding of parameters of best fit model for simulation purposes
25  mu=J(1); %empirical drift of simplified model used for jump inference
26  lamb=J(2);%Jump intensity
27  V=J(3);%Variance of jump sizes
28  mu_bar=J(4);%mean of empirical drift
29  sg_bar=J(5);%mean of empirical volatility
30  del=sqrt(log(V+1));
31  ga=-((del^2)/2); %to keep the mean jump size zero
32  plamb=1-(exp(-lamb*dt)); %probability of observing at least one jump in dt time–
        length
33  alpha=(0.5)*10^40; % alpha=(0.5)*10^40 gives \hat{p}=1.0122%
34  ph=min(1,alpha*(dt^(log(1/dt)))); %\hat{p} value
```

```matlab
35  g=sqrt(dt)*norminv((1+((1-ph)^(1/N)))/2); %g is \gamma
36
37  %For each j, a simulation and accuracy of jump classification is computed. Then
        average accuracy is computed for each beta.
38  W=zeros(1,N+1);
39  W(1)=0;
40  for i=1:N2       %Brownian motion
41      u1=rand(); %by Box Muller Method
42      u2=rand();
43      W(2*i)=W(2*i-1)+sqrt(dt*(-2)*log(1-u1))*cos(2*pi*u2);
44      W(2*i+1)=W(2*i)+sqrt(dt*(-2)*log(1-u1))*sin(2*pi*u2);
45  end
46
47  S_u=zeros(1,N); %Asset time series initialization
48  S_u=s(1);        %Initial Asset price
49  Xi=zeros(1,N);
50  for i=1:N-1      %Simulation using above W and following Xi.
51      u1=rand();
52      if u1 <= plamb   % then jump happens
53          u1=rand();    % Generating Jump Size (Merton Model)
54          u2=rand();    % Jump size is LogNormal -1
55          Xi(i)=exp(ga+del*sqrt((-2)*log(1-u1))*cos(2*pi*u2))-1;
56      else              % else jump does not occur
57          Xi(i)=0;      % so Xi(i) =0
58      end
59      S_u(i+1)=S_u(i)*(1+mu_bar*dt+sg_bar*(W(i+1)-W(i))+Xi(i));
60  end                    %Simulation is complete.
61
62  ret_cu=sr(S_u);%This is the simple return series obtained from the simulation of
        uni-regime MJD model
63
64  ret_cu=sort(ret_cu);%sorting of simple return series
65
66  sig_m=sg_bar*[1-eps,1,1+eps];%empirical volatility vector for simulation of  best
        fit TRMJD model
67
68  mu_m=mu_bar*ones(1,3);%empirical drift vector for simulation of best fit TRMJD
        model
69  x=[];
70  x=mrk3(N,dt,a,l_m);%simulation of ternary regime Markov process using the
        instantaneous transition rate of best fit TRMJD model
71  W=zeros(1,N+1);
```

```matlab
72  W(1)=0;
73
74  for  i =1:N2        %Brownian  motion
75      u1=rand ( ) ;  %by  Box  Muller  Method
76      u2=rand ( ) ;
77      W(2* i )=W(2* i −1)+sqrt ( dt *(−2)* log (1−u1 ) ) * cos (2* pi *u2 ) ;
78      W(2* i +1)=W(2* i )+sqrt ( dt *(−2)* log (1−u1 ) ) * sin (2* pi *u2 ) ;
79  end
80
81  S_m=zeros ( 1 ,N) ; %Asset  time  series  initialization
82  S_m(1)=s ( 1 ) ;        %Initial  Asset  price
83  Xi=zeros ( 1 ,N) ;
84  for  i =1:N−1        %Simulation  using  above  W and  following  Xi .
85      u1=rand ( ) ;
86      if  u1 <= plamb    % then  jump  happens
87          u1=rand ( ) ;    % Generating  Jump  Size  (Merton  Model)
88          u2=rand ( ) ;    % Jump  size  is  LogNormal −1
89          Xi ( i )=exp ( ga+del * sqrt ((−2)* log (1−u1 ) ) * cos (2* pi *u2 ) )−1;
90      else              % else  jump  does  not  occur
91          Xi ( i )=0;      % so  Xi ( i )  =0
92      end
93      S_m( i +1)=S_m( i ) *(1+mu_m( x ( i ) ) * dt+sig_m ( x ( i ) ) *(W( i +1)−W( i ) )+Xi ( i ) ) ;%simulation
               of  the  TRMJD  model
94  end                    %Simulation  is  complete .
95
96  ret_cm=sr (S_m) ;   %This  is  the  simple  return  series  obtained  from  the  simulation  of
        best  fit  TRMJD  model
97  ret_cm=sort ( ret_cm ) ;%sorting  of  simple  return  series
98   max_r=max(max( ret ) ) ;%maximum  of  the  empirical  return  series
99   min_r=min ( min ( ret ) ) ;%maximum  of  the  empirical  return  series
100  xr=linspace ( min_r , max_r ,11001) ;%generation  of  a  mesh  of  equispaced  points  between
        max_r  and  min_r  for  obtaining  the  empirical  CDF(eCDF)  ( of  empirical  and
        theoretical  models )  and  the  L2  norm  of  empirical  CDF
101  x2=diff ( xr ) ;%difference  of  consecutive  elements  of  the  generated  mesh  vector
102  x1=xr ( 1 :end−1) ;
103  f1 =( invprctile ( ret , x1 ) ) /100;%empirical  eCDF
104  f2 =( invprctile ( ret_cu , x1 ) ) /100;%Uni−regime  MJD  model  eCDF
105  f3 =( invprctile ( ret_cm , x1 ) ) /100;%TRMJD  model  eCDF
106  %calculating  the  square  if  the  difference  of  elements  of  same  index  of  different
        eCDF' s
107  f_21 =( f2−f1 ) .^2;
108  f_31 =( f3−f1 ) .^2;
```

62

```matlab
109
110  %Kolmogorov−Smirnov (K−S Test)
111  len1=size(ret,2);%length of return time series
112  len2=size(ret_cu,2);%length of uni−regime MJD return series
113  len3=size(ret_cm,2);%length TRMJD return series
114
115  D(1)=(max(abs(f2−f1)))/(sqrt((len1+len2)/(len1*len2)));%K−S Test statistic of the
         eCDF'S of return time series and uni−regime MJD model
116  D(2)=(max(abs(f3−f1)))/(sqrt((len1+len3)/(len2*len3)));%K−S Test statistic of  of
         return time series and TRMJD model
117  D(3)=max(abs(f3−f2))/(sqrt((len2+len3)/(len2*len3)));%K−S Test statistic  of uni−
         regime MJD and TRMJD
118
119  L2(1)=sqrt(sum(f_21.*x2));%L2 error of  uni−regime MJD
120  L2(2)=sqrt(sum(f_31.*x2));%L2 error of TRMJD
121
122  filename1='L2.xlsx';
123  sheet=1;
124  xlswrite(filename1,L2,sheet,'Am:Bm');
125  filename2='KStest.xlsx';
126  xlswrite(filename2,D,sheet,'Am:Cm');
```

A.6 User Defined Functions Used in the Main Code

A.6.1 Simulation of Markov Chain

```matlab
function M=markovfun(L,TPM,dt,Ft)

    CPM=transpose(cumsum(transpose(TPM)));%cumulative probability matrix
    X(1)=1;%initial state of the Markov chain
    a=0;
    m=ceil(Ft/dt);%no time points
    j=0;
    while ceil(a/dt)<m
        j=j+1;
        T(j)=exprnd(1/L(X(j)));
        b=a+T(j);%overall time spent till state X(j)
        for i=ceil(a/dt)+1:min(ceil(b/dt),m)
            M(i)=X(j);% Markov chain state
        end
        if ceil(b/dt)>m
            break
        else
            a=b;
            cumdist=CPM(X(j),:);
            r = rand();
            X(j+1)=find(cumdist>r,1);%next state of Markov chain
        end
    end
```

A.6.2 Simple Return

```matlab
function ret=sr(a)
n=size(a,2);
    ret=zeros(1,n-1);
    for i=1:(n-1)
        ret(i)=((a(i+1)-a(i))/a(i));%calculation of simple return of time series
            data 'a'
    end
end
```

A.6.3   Squeeze Durations i.e Corresponding to pth Percentile

```matlab
function dura=dura(a,p)

    n=size(a,2);
    P=prctile(a,p);
    flag_1=1;
    transition_1=[];%initialization
    %calculating durations
    for j=1:n
        if flag_1*a(j)<flag_1*P
            transition_1=[transition_1,j];
            flag_1=-flag_1;
        end
    end
    transition=transition_1;
    Dura=diff(transition);
    dura=Dura(1:2:end);% squeeze durations
    end
```

A.6.4   Expansion Durations i.e Corresponding to (100-p)th Percentile

```matlab
function dura_mi=dura_mi(a,p)
n=size(a,2);
Q=prctile(a,(100-p));%calculating (100-p)th percentile
    transition_2=[];%initialization
    flag_2=1;
    %calculation of durations
    for k=1:n
        if flag_2*a(k)>flag_2*Q
            transition_2=[transition_2,k];
            flag_2=-flag_2;
        end
    end
    transition_m=transition_2;
    Dura_m=diff(transition_m);
    dura_mi=Dura_m(1:2:end);%expansion durations
    end
```

A.6.5 Asset Price Simulation by a GBM Model/uni-regime MJD after removal of jump term

```
1   function St=gsm(S,dt,N, mu,sg)
2        %'mu' is the drift and 'sg' is the volatility
3        St=[];%initialization
4        St(1)=S;%initial asset price
5        sdt=sqrt(dt);
6        a=0
7        for i=2:N
8            w=normrnd(0,sdt);
9            a=mu*dt+sg*w-0.5*(sg^2)*dt;
10           St(i)=St(i-1)*exp(a); %calculation of asset price
11           end
12  end
```

A.6.6 Asset Price Simulation by an MMGBM Model/ TRMJD model after removal of jump term

```
1   function St_m=mgbm_1(S,N,dt,a,l_m,mu_m,sg_1)
2   x(1)=2;%initial state of Markov chain
3   for i=1:N
4       h=(((a)^2)/(((a)^2)+1));%calculation of  parameter for 'eta_i' Beroulli Random
                variable
5       z=binornd(1,h);%generating 'eta_i' Bernoulli random variable
6       Q=binornd(1,((l_m(x(i)))*dt));
7       x(i+1)=x(i)+((2-x(i))+((kd(x(i)))*((-1)^z)))*Q;% generation of next state in
                the Markov chain
8   end
9   a_1=0;%initialisation
10    St_m(1)=S;%initial asset price
11    for j=2:N
12                  w_1=normrnd(0,sqrt(dt));
13                  a_1=((mu_m(x(j)))*dt)+((sg_1(x(j)))*w_1)-((0.5*((sg_1(x(j)))^2))*dt
                    );
14                   St_m(j)=St_m(j-1)*exp(a_1);%generation of asset price from
                        MMGBM model
15        end
16  end
```

A.6.7 g_b Function Used for Calculating Discriminating Statistics

```matlab
function g_b=g_b(x,B)
    g_b=max((min(x,(B-x))/B),0); %g_b function defined in the calculation of
        discriminating statistics
end
```

A.6.8 Kronecker Delta Function $\delta_{(2,j)}$

```matlab
% Kronecker delta function of state '2' of the Markov chain
function kd=kd(s)
    if s==2
        kd=1;
    elseif s==1
        kd=0;
    elseif s==3
        kd=0;
    end
end
```

A.6.9 Discrete Form of Ternary Regime switching Markov Chain

```matlab
function x=mrk3(N,dt,a,l_m)
x(1)=2;%initialization
for i=1:N
    h=(((a)^2)/(((a)^2)+1));%calculation of parameter for 'eta_i'Bernoulli random
        variable
    z=binornd(1,h);%generating 'eta_i' Bernoulli random variable
    Q=binornd(1,((l_m(x(i)))*dt));%P_i Bernoulli random variable
    x(i+1)=x(i)+((2-x(i))+((kd(x(i)))*((-1)^z)))*Q;% generation of next state in
        the Markov chain
end
```

Bibliography

[1] Basak, Gopal K., Mrinal K. Ghosh, and Anindya Goswami. Risk minimizing option pricing for a class of exotic options in a Markov-modulated market. Stochastic Analysis and Applications 29.2 (2011), 259-281.

[2] Bo, Lijun, Yongjin Wang, and Xuewei Yang. Markov-modulated jumpdiffusions for currency option pricing. Insurance: Mathematics and Economics 46.3 (2010), 461-469.

[3] Fan, K., Shen, Y., Siu, T. K., & Wang, R. Pricing foreign equity options with regime-switching. Economic Modelling, 37(2014), 296-305.

[4] Jobert, Arnaud, and Leonard CG Rogers. Option pricing with Markov-modulated dynamics. SIAM Journal on Control and Optimization 44.6 (2006), 2063-2078.

[5] Li, Jinzhi, and Shixia Ma. Pricing options with credit risk in Markovian regime-switching markets. Journal of Applied Mathematics 2013(2013), 621371, 9 pages.

[6] Lian, Yu-Min, Jun-Home Chen, and Szu-Lang Liao. Option pricing on foreign exchange in a Markov-modulated, incomplete- market economy. Finance Research Letters 16 (2016), 208-219.

[7] Papin, Timothee, and Gabriel Turinici. Prepayment option of a perpetual corporate loan: the impact of the funding costs. International Journal of Theoretical and Applied Finance 17.4(2014), 1450028.

[8] Siu, Tak Kuen, Hailiang Yang, and John W. Lau. Pricing currency options under two-factor Markov-modulated stochastic volatility models. Insurance: Mathematics and Economics 43.3 (2008), 295-302.

[9] Su, Xiaonan, Wensheng Wang, and Kyo-Shin Hwang. Risk-minimizing option pricing under a Markov-modulated jump- diffusion model with stochastic volatility. Statistics & Probability Letters 82.10 (2012), 1777-1785.

[10] Swishchuk, Anatoliy, Maksym Tertychnyi, and Robert Elliott. Pricing currency derivatives with Markov-modulated Lvy dynamics. Insurance: Mathematics and Economics 57 (2014), 67-76.

[11] Wang, W., Jin, Z., Qian, L., and Su, X. Local risk minimization for vulnerable European contingent claims on nontradable assets under regime switching models. Stochastic Analysis and Applications 34.4 (2016), 662-678.

[12] Yuen, Fei Lung, and Hailiang Yang. Option pricing in a jump-diffusion model with regime switching. ASTIN Bulletin: The Journal of the IAA 39.2 (2009), 515-539.

[13] Di Masi, Giovanni B., Yu M. Kabanov, and Wolfgang J. Runggaldier. Mean-variance hedging of options on stocks with Markov volatilities. Theory of Probability & Its Applications 39.1 (1995), 172-182.

[14] Hamilton, James D. A new approach to the economic analysis of nonstationary time series and the business cycle. Econo- metrica: Journal of the Econometric Society (1989), 357-384.

[15] Heston Stephen L., A Closed-Form Solution for Options with Stochastic Volatility with Applications to Bond and Currency Options, Rev. Finan. Stud., 6(1993), no. 2, 327-343.

[16] Stéphane Goutte, Amine Ismail, Huyên Pham. Regime-switching Stochastic Volatility Model: Estimation and Calibration to VIX options. 2017. ffhal-01212018v2f

[17] Black F. and Scholes M., The pricing of options and corporate liability, Journal of Political Economy, Vol. 81, No. 3 (1973), 637-659.

[18] Siu, Tak Kuen Fair valuation of participating policies with surrender options and regime switching. Insurance Math. Econom. 37 (2005), no. 3, 533–552. (Reviewer: Ali Süleyman Üstünel) 60H30 (60G40 60H10 91B28 91B30)

[19] Boyle, Phelim; Draviam, Thangaraj. Pricing exotic options under regime switching. Insurance Math. Econom. 40 (2007), no. 2, 267–282. 91B28

[20] Elliott, Robert J.; Siu, Tak Kuen; Badescu, Alexandru On pricing and hedging options in regime-switching models with feedback effect. J. Econom. Dynam. Control 35 (2011), no. 5, 694–713. (Reviewer: Hsien-Jen Lin) 91G20

[21] Guo, Xin Information and option pricings. Quant. Finance 1 (2001), no. 1, 38–44. (Reviewer: Dave Furth) 91B28 (91B70)

[22] Deshpande, Amogh (6-IIS); Ghosh, Mrinal K. (6-IIS) Risk minimizing option pricing in a regime switching market. (English summary) Stoch. Anal. Appl. 26 (2008), no. 2, 313–324. 91B28 (60G44 91B70)

[23] Mamon, Rogemar S.; Rodrigo, Marianito R. Explicit solutions to European options in a regime-switching economy. Oper. Res. Lett. 33 (2005), no. 6, 581–586. (Reviewer: Jan Kallsen) 91B28

[24] Chan, Terence. Pricing contingent claims on stocks driven by Lévy processes. Ann. Appl. Probab. 9 (1999), no. 2, 504–528. (Reviewer: Rüdiger Kiesel) 91B28

[25] Kou, S. G. A jump diffusion model for option pricing. Management Science 48, 1086-1101, (2002).

[26] Elliott, Robert J.; Siu, Tak Kuen; Chan, Leunglung; Lau, John W. Pricing options under a generalized Markov-modulated jump-diffusion model. Stoch. Anal. Appl. 25 (2007), no. 4, 821–843. (Reviewer: Volkert Paulsen) 60H30 (60G44 60H10 91B28)

[27] Su, Xiaonan Wang, Wensheng; Hwang, Kyo-Shin Risk-minimizing option pricing under a Markov-modulated jump-diffusion model with stochastic volatilit". Statist. Probab. Lett. 82 (2012), no. 10, 1777–1785. 60H30 (60J75 91B70 91G20)

[28] Yoshio Miyahara & Alexander Novikov, 2001. "Geometric Lévy Process Pricing Model, " Research Paper Series 66, Quantitative Finance Research Centre, University of Technology, Sydney.

[29] P. Nowak and M. Pawłowski, "Option Pricing With Application of Levy Processes and the Minimal Variance Equivalent Martingale Measure Under Uncertainty, " in IEEE Transactions on Fuzzy Systems, vol. 25, no. 2, pp. 402-416, April 2017, doi: 10.1109/TFUZZ.2016.2637372.

[30] Sepp, Artur, Pricing Options on Realized Variance in the Heston Model with Jumps in Returns and Volatility (April 21, 2008). Journal of Computational Finance, Vol. 11, No. 4, pp. 33-70, 2008

[31] Figueroa-Lopez, José E. and Mancini, Cecilia, Optimum Thresholding Using Mean and Conditional Mean Square Error (August 7, 2017). Available at SSRN: https://ssrn.com/abstract=3047108 or http://dx.doi.org/10.2139/ssrn.3047108

[32] George J. Jiang, Estimation of Jump-Diffusion Processes Based on Indirect Inference, IFAC Proceedings Volumes, Volume 31, Issue 16, 1998, Pages 385-390, ISSN 1474-6670, https://doi.org/10.1016/S1474-6670(17)40510-6.

[33] Das, Milan & Goswami, Anindya & Rajani, Sharan. (2019). Inference of Binary Regime Models with Jump Discontinuities.

[34] Abramowitz, Milton, and Irene A. Stegun, eds. Handbook of mathematical functions with formulas, graphs, and mathematical tables. Vol. 55. US Government printing office, 1948.

[35] Aït-Sahalia, Yacine. Disentangling diffusion from jumps. Journal of financial economics 74.3 (2004): 487-528.

[36] Bo, Lijun; Yongjin Wang; and Xuewei Yang. Markov-modulated jump-diffusions for currency option pricing. Insurance: Mathematics and Economics 46.3 (2010): 461-469.

[37] Bulla, Jan; and Ingo Bulla. Stylized facts of financial time series and hidden semi-Markov models. Computational Statistics & Data Analysis 51.4 (2006): 2192-2209.

[38] Cont, Rama; and Tankov, Peter. Financial modelling with jump processes. Chapman and Hall/CRC, 2003.

[39] Eraker, Bjørn; Michael Johannes; and Nicholas Polson. The impact of jumps in volatility and returns. The Journal of Finance 58.3 (2003): 1269-1300.

[40] Jacod, Jean. Asymptotic properties of realized power variations and related functionals of semimartingales. Stochastic processes and their applications 118.4 (2008): 517-559.

[41] Jobert, Arnaud; and Rogers, Leonard CG. Option pricing with Markov-modulated dynamics. SIAM Journal on Control and Optimization 44.6 (2006): 2063-2078.

[42] Madan, Dilip B.; Peter P. Carr; and Eric C. Chang. The variance gamma process and option pricing. Review of Finance 2.1 (1998): 79-105.

[43] Mancini, Cecilia. Non-parametric Threshold Estimation for Models with Stochastic Diffusion Coefficient and Jumps. Scandinavian Journal of Statistics 36 (2009): 270-296.

[44] Merton, Robert C. Option pricing when underlying stock returns are discontinuous. Journal of financial economics 3.1-2 (1976): 125-144.

[45] Schreiber, Thomas; and Andreas Schmitz. Surrogate time series. Physica D: Nonlinear Phenomena 142.3 (2000): 346-382.

[46] Theiler, James; and Dean Prichard. Constrained-realization Monte-Carlo method for hypothesis testing. Physica D: Nonlinear Phenomena 94.4 (1996): 221-235.

[47] Theiler, James; Eubank, S.; Longtin, A.; Galdrikian, B.; and Farmer, J. D. Testing for nonlinearity in time series: the method of surrogate data. Physica D: Nonlinear Phenomena, (1992) 58(1-4): 77-94.

[48] Theiler, James; and Dean Prichard. Constrained-realization Monte-Carlo method for hypothesis testing. Physica D: Nonlinear Phenomena 94.4 (1996): 221-235.

[49] Merton, Robert C. Option pricing when underlying stock returns are discontinuous. Journal of Financial economics 3.1-2 (1976): 125-144.

[50] Milan Kumar Das and Anindya Goswami, 2019. "Testing of binary regime switching models using squeeze duration analysis," International Journal of Financial Engineering (IJFE), World Scientific Publishing Co. Pte. Ltd., vol. 6(01), pages 1-20, March.